

# RobustCalibration: Robust Calibration of Computer Models in R

Mengyang Gu

**Abstract** Two fundamental research tasks in science and engineering are forward predictions and data inversion. This article introduces a recent R package **RobustCalibration** for Bayesian data inversion and model calibration by experiments and field observations. Mathematical models for forward predictions are often written in computer code, and they can be computationally expensive slow to run. To overcome the computational bottleneck from the simulator, we implemented a statistical emulator from the **RobustGaSP** package for emulating both scalar-valued or vector-valued computer model outputs. Both posterior sampling and maximum likelihood approach are implemented in the **RobustCalibration** package for parameter estimation. For imperfect computer models, we implement Gaussian stochastic process and the scaled Gaussian stochastic process for modeling the discrepancy function between the reality and mathematical model. This package is applicable to various types of field observations, such as repeated experiments and multiple sources of measurements. We discuss numerical examples of calibrating mathematical models that have closed-form expressions, and differential equations solved by numerical methods.

## Introduction

Science and engineering are increasingly attempting to model complex behaviors of processes by mathematical models, which are often written in computer code. These mathematical models are thus often called *computer models* or *simulators*. Given a set of parameters and initial conditions, computer models are widely used to simulate physical, engineering or human processes (Sacks et al., 1989). The initial conditions and model parameters may be unknown or uncertain in practice. Calibrating the computer models based on real experiments or observations is one of the fundamental tasks in science and engineering, widely known as the *data inversion* or *model calibration*.

We follow the notation in Bayarri et al. (2007a) for defining the model calibration problem. Let the real-valued field observation be  $y^F(\mathbf{x})$  with  $p_x$ -dimensional observable input vector  $\mathbf{x}$ . The field observation is often decomposed by  $y^F(\mathbf{x}) = y^R(\mathbf{x}) + \epsilon$ , where  $y^R(\cdot)$  denotes a function of unknown reality, and  $\epsilon$  denotes the noise. The superscript ‘F’ and ‘R’ denote field observations (or experimental data) and reality, respectively. Scientists often model the unknown reality by a computer model, denoted by  $f^M(\mathbf{x}, \boldsymbol{\theta})$  at  $p_x$ -dimensional observable input  $\mathbf{x}$ , and  $p_\theta$ -dimensional calibration parameters  $\boldsymbol{\theta}$ , unobservable from the experiments, with superscript ‘M’ denoting the computer model.

When the computer model describes the reality perfectly, the field observation can be written as:

$$y^F(\mathbf{x}) = f^M(\mathbf{x}, \boldsymbol{\theta}) + \epsilon, \quad (1)$$

where  $\epsilon$  is zero-mean Gaussian noise. We call the calibration method by equation (1) the *no-discrepancy calibration*.

When computer models are imperfect, the following statistical framework of model calibration is widely used:

$$y^F(\mathbf{x}) = f^M(\mathbf{x}, \boldsymbol{\theta}) + \delta(\mathbf{x}) + \epsilon, \quad (2)$$

where  $\delta(\cdot)$  is the unobservable discrepancy between the mathematical model and reality. Equation (2) implies that the reality can be written as  $y^R(\mathbf{x}) = f^M(\mathbf{x}, \boldsymbol{\theta}) + \delta(\mathbf{x})$  at any observable input  $\mathbf{x} \in \mathcal{X}$ . The model calibration framework has been studied extensively. In Kennedy and O’Hagan (2001), the discrepancy function  $\delta(\cdot)$  is modeled via a Gaussian stochastic process (GaSP). The predictive accuracy based on the joint model of calibrated computer model and discrepancy was found to be better compared to using the computer model or discrepancy model for prediction alone. We call this method the *GaSP Calibration*. The GaSP calibration has been applied in a wide range of studies for continuous and categorical variables (Bayarri et al., 2007a; Higdon et al., 2008; Paulo et al., 2012; Chang et al., 2016). Both no-discrepancy calibration and GaSP calibration are implemented in the **RobustCalibration** package. Furthermore, historical data may be used for reducing the parameter space (Williamson et al., 2013).

When the discrepancy function is modeled by the GaSP, the calibrated computer model output can be far from the observations in terms of  $L_2$  distance (Arendt et al., 2012; Tuo and Wu, 2016), since a large proportion of the variability of the data can be explained by discrepancy function. To solve this problem, we implemented the scaled Gaussian stochastic process (S-GaSP) calibration, or *S-GaSP Calibration* in the **RobustCalibration** package. The S-GaSP model of discrepancy function was first

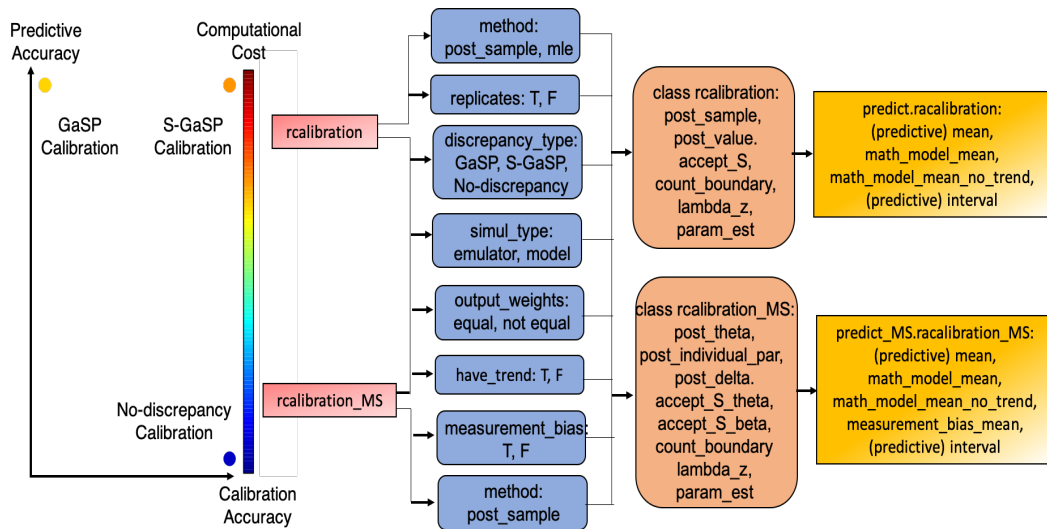


**Figure 1:** Schematic overview of the **RobustCalibration** package. The left panel show the predictive accuracy based on calibrated computer model and discrepancy versus calibration accuracy by calibrated computer model, evaluated by the  $L_2$  loss to reality. The right panel give an overview of the major functions and classes in **RobustCalibration**. The calibration and calibration\_MS in red boxes are the main function for parameter estimation for observations from single sources and from multiple sources, respectively. Some main arguments of these two functions are given in the blue boxes. The orange boxes give the object classes and main slots that will be created after calling calibration or calibration\_MS functions. Finally, the object classes can be used for predicting the reality, either based on calibrated computer model and discrepancy, or by calibrated computer model alone.

introduced in Gu and Wang (2018), where a new probability measure of the random  $L_2$  loss between the computer model and reality was derived, such that more prior probability mass of the  $L_2$  loss is placed on small values. Consequently, the calibrated computer model by the S-GaSP fits the reality better in terms of  $L_2$  loss than the GaSP calibration. Theoretical properties of S-GaSP, such as associated reproducing kernel Hilbert space and convergence rates were studied in Gu et al. (2018b).

A few recent approaches aim to minimize the the  $L_2$  distance between the reality and computer model (Tuo and Wu, 2015, 2016; Wong et al., 2017), where the reality and discrepancy function are often estimated in two steps separately. The S-GaSP calibration bridges the two-step  $L_2$  calibration to the GaSP calibration. Compared with the two-step approaches, parameters and discrepancy  $(\theta, \delta(\cdot))$  are estimated in GaSP calibration and S-GaSP calibration jointly, and the uncertainty of these estimation can be obtained based on the likelihood function of the sampling model. Furthermore, compared with the orthogonal calibration model (Plumlee, 2017), the S-GaSP process places more prior mass on the small  $L_2$  loss, instead of all extreme points of this loss functions. Indeed, a small  $L_2$  loss indicates that calibrated computer model can approximately reproduce the reality.

Figure 1 gives a schematic overview of the **RobustCalibration** package. We consider two criteria by predicting the reality: using both calibrated computer model and discrepancy (predictive accuracy), and calibrated computer model alone (calibration accuracy), both evaluated in terms of the  $L_2$  loss. The left panel gives comparison of accuracy and computational cost between the implemented methods. The no-discrepancy is the fastest, as the main computational cost lies on approximating computer models by emulators or by numerical methods. The GaSP and S-GaSP calibration have the same computational order, due to inverting the covariance matrix of the field data based on Cholesky decomposition. Because of the inclusion of the model of discrepancy, the predictive accuracy by GaSP and S-GaSP is the highest.

The **RobustCalibration** package can handle model calibration and prediction at a wide range of settings shown in blue boxes in Figure 1. First of all, both the posterior sampling and maximum likelihood estimator (MLE) were implemented in the `rcalibration` function. Users can choose no-discrepancy calibration and two different choices of modeling the discrepancy function (GaSP or S-GaSP) in modeling. Calibration models for replicates or repeated experiments (Bayarri et al., 2007b) based on sufficient statistics are also implemented. The computational cost is much smaller than direct implementation. For all scenarios, posterior sampling through the Markov chain Monte Carlo (MCMC) algorithm was implemented for Bayesian data inversion. Besides, we implement the MLE as a fast approach to obtain the point estimator of parameters for model calibration by a single source of data. After calling the `rcalibration` function, a "rcalibration" class (shown in the upper orange box)

will be created, and prediction can be computed by calling the `predict.calibration` function (upper yellow box). Motivated by geophysical applications (Anderson et al., 2019), the `rcalibration_MS` function allows user to calibrate computer models using multiple sources of data or multiple types of observations, such as multiple images and time series. A “`rcalibration_MS`” class will be created by the `rcalibration_MS` function, and `predict_MS.rcalibration_MS` can be called for predictions.

Some computer models can be expensive to run, as the computer model outputs are typically numerical solutions of a system of differential equations. When computer model is slow, a statistical emulator is often used for approximating computationally expensive computer model. The GaSP emulator is a well-developed framework for emulating computationally expensive computer models and it was implemented in a few R packages, e.g. **DiceKriging** (Roustant et al., 2012), **GPfit** (MacDonald et al., 2015) and **RobustGaSP** (Gu et al., 2019). Here we use `rgasp` and `ppgasp` in **RobustGaSP** for emulating computer models with scalar-valued and vector-valued output, respectively.

Building packages for Bayesian model calibration is more complicated than packages in statistical emulator, as both field observations and computer models are integrated. A few statistical packages are available for Bayesian model calibration, such as **BACCO** (Hankin, 2005), **SAVE** package (Palomo et al., 2015), and **CaliCo** (Carmassi et al., 2018). The **CaliCo** package, for example, integrates **DiceKriging** for emulating computational expensive simulations. It offers different types of diagnostic plots based on **ggplot2** (Wickham, 2011), and different prior choices of the parameters. The **BACCO** and **SAVE** consider the GaSP model of the discrepancy function (Kennedy and O’Hagan, 2001), and they emulate slow computer models by GaSP emulators as well.

Although a large number of studies were developed for Bayesian model calibration, to the authors’ best knowledge, many methods implemented in **RobustCalibration** were not implemented in another software package before. We highlight a few unique features of the **RobustCalibration** package. First of all, we allow users to specify different types of output of field observations, for different scenarios through the `output` argument in the `rcalibration` function. The simplest scenario is a vector output. We allow users to input a matrix type or a list for fields observations with the same or different number of replications, respectively. Efficient computation based on sufficient statistics was implemented for model calibration with replications, and it can improve the computation up to  $k^3$  times, where  $k$  is the number of repeated experiments. Second, models with different types and from multiple sources are can also be integrated for model calibration, based on the the `calibration_MS` function. Third, we implemented emulators for approximating expensive computer models with both scalar-valued and vector-valued outputs. To the author’s knowledge, emulators for vector-valued outputs, especially at a large number of temporal or spatial coordinates, were not integrated in other packages for Bayesian model calibration. Here we use the parallel partial Gaussian stochastic process (PP-GaSP) emulator from **RobustGaSP** (Gu et al., 2019) as a computationally scalable emulator of vector-valued output. Furthermore, when computer models are imperfect, users can choose no-discrepancy, GaSP and S-GaSP models of discrepancy function. Finally, both posterior samples and MLE were implemented and made available by the `method` argument in the `rcalibration` function.

The rest of the paper is organized below. We first introduce the statistical framework for model calibration problem. Numerical examples and code will be provided along the methodology to illustrate the implemented methods in the **RobustCalibration** package. Then we give an overview of the architecture of the package, and we provide additional numerical examples for comparison. Closed form expressions of likelihood functions, derivatives and posterior distributions and computational algorithms are provided in Appendix.

## Statistical framework

We introduce the statistical framework in the this section, starting with the simplest method: no-discrepancy calibration. Then we discuss two models of discrepancy functions. For any kernel function uses in GaSP calibration, S-GaSP provides a transformed kernel from scaling the prior of the random  $L_2$  loss between reality and computer models. We then introduce model calibration with repeated experiments, the statistical emulator for approximating computationally expensive computer models. Model calibration by data from multiple sources will be discussed at the end. Numerical examples and code from the **RobustCalibration** package will be provided along with the introduction.

### No-discrepancy calibration

First, suppose we obtain a vector of real-valued field observations  $\mathbf{y}^F = (y^F(\mathbf{x}_1), \dots, y^F(\mathbf{x}_n))^T$  at  $n$  observable inputs. The corresponding computer model output is denoted by  $\mathbf{f}_\theta^M = (f^M(\mathbf{x}_1, \theta), \dots, f^M(\mathbf{x}_n, \theta))^T$  for any calibration parameters  $\theta$ . Further assume the vector of measurement noise independently follows Gaussian distributions  $\epsilon \sim \mathcal{MN}(0, \sigma_0^2 \Lambda)$ , where the covariance of the noise is diagonal with

the  $i$ th term being  $\sigma_0^2 \Lambda_{ii}$  and  $\mathcal{MN}$  denote the multivariate Gaussian distribution. Here noises are independent and we will consider correlated noises based on multiple sources of data later. In the default setting,  $\sigma_0^2$  is estimated by data and  $\mathbf{\Lambda} = \mathbf{I}_n$ , where  $\mathbf{I}_n$  is an identity matrix with  $n$  dimensions. Users can specify the inverse of the diagonal terms of  $\mathbf{\Lambda}$  by the `output_weights` argument in `rcalibration` and `rcalibration_MS` functions, as variances of measurement errors can be different. We assume the diagonal matrix  $\mathbf{\Lambda}$  is given in this section.

For a no-discrepancy calibration model in (1), the MLE of the variance of the noise is  $\hat{\sigma}_0^2 = S_0^2/n$  with  $S_0^2 = (\mathbf{y}^F - \mathbf{f}_\theta^M)^T \mathbf{\Lambda}^{-1} (\mathbf{y}^F - \mathbf{f}_\theta^M)$ . The likelihood function is given in Appendix. As  $\mathbf{\Lambda}$  is a diagonal matrix with diagonal terms denoted as  $\Lambda_{ii} := 1/w_i$ , the profile likelihood follows

$$\mathcal{L}(\boldsymbol{\theta} \mid \hat{\sigma}_0^2) \propto \left\{ \sum_{i=1}^n w_i \left( y^F(\mathbf{x}_i) - f^M(\mathbf{x}_i, \boldsymbol{\theta}) \right)^2 \right\}^{-n/2},$$

where  $w_i = 1$  is used in the default scenario. Note that maximizing the profile likelihood of a no-discrepancy model is equivalent to minimize  $w_i \left( y^F(\mathbf{x}_i) - f^M(\mathbf{x}_i, \boldsymbol{\theta}) \right)^2$ , the weighted squared error loss on observed inputs. We numerical find  $\boldsymbol{\theta}$  by the low-storage quasi-Newton optimization method (Nocedal, 1980; Liu and Nocedal, 1989) implemented in `lbfgs` function in the `nloptr` package (Ypma (2014)) for optimization. We allow users to input derivatives of  $f^M$  with respect to  $\boldsymbol{\theta}$  in numerical optimization. If the derivative is not given, the numerical derivative will be computed.

In **RobustCalibration** package, we allow users to specify the trend or mean function modeled as  $\mu(\mathbf{x}_i) = \mathbf{h}(\mathbf{x})\boldsymbol{\theta}_m = \sum_{t=1}^q h_t(\mathbf{x})\theta_{m,t}$  for any  $\mathbf{x}$ , where  $\boldsymbol{\theta}_m = (\theta_{m,1}, \dots, \theta_{m,q})^T$  is a vector of trend parameters. The MLE of the trend parameter is the least square estimator  $\hat{\boldsymbol{\theta}}_m^{LS} = (\mathbf{H}^T \mathbf{\Lambda}^{-1} \mathbf{H})^{-1} \mathbf{H}^T \mathbf{\Lambda}^{-1} (\mathbf{y}^F - \mathbf{f}_\theta^M)$  with  $\mathbf{H} = (\mathbf{h}^T(\mathbf{x}_1), \dots, \mathbf{h}^T(\mathbf{x}_n))^T$  being an  $n \times q$  matrix of the mean basis. It is easy to show maximizing the profile likelihood of a no-discrepancy model with a mean function is equivalent to minimize the the squared error loss:

$$\hat{\boldsymbol{\theta}}_{LS} = \operatorname{argmin}_{\boldsymbol{\theta}} \sum_{i=1}^n w_i \left( y^F(\mathbf{x}_i) - f^M(\mathbf{x}_i, \boldsymbol{\theta}) - \mathbf{h}(\mathbf{x}_i) \hat{\boldsymbol{\theta}}_m^{LS} \right)^2.$$

After calling the `rcalibration` function with `method='mle'`, the point estimator  $\hat{\boldsymbol{\theta}}_{LS}$  is recorded in the slot `param_est` in the `rcalibration` class. The MLE is a computationally cheap way to obtain estimation of calibration parameter  $\boldsymbol{\theta}$ . After obtaining the MLE, we can use a plug the MLE into the computer model to compute the prediction of reality:  $f^M(\mathbf{x}_i, \hat{\boldsymbol{\theta}}) + h(\mathbf{x}_i) \hat{\boldsymbol{\theta}}_m^{LS}$ . Computing the predictions, predictive interval of the mean or observations was implemented in the `predict` function.

The uncertainty of the MLE can be hard to obtain, and the plug-in estimator does not propagate the uncertainty in prediction. To overcome this problem, we implement the MCMC algorithm for Bayesian inference. The posterior distributions follow

$$p(\boldsymbol{\theta}_m, \sigma_0^2, \boldsymbol{\theta} \mid \mathbf{y}^F) \propto p(\mathbf{y}^F \mid \boldsymbol{\theta}, \boldsymbol{\theta}_m, \sigma_0^2) \pi(\boldsymbol{\theta}) \pi(\boldsymbol{\theta}_m, \sigma_0^2). \quad (3)$$

We assume an objective prior for the mean and variance parameters  $\pi(\boldsymbol{\theta}, \sigma_0^2) \propto 1/\sigma_0^2$ . The posterior distribution  $p(\boldsymbol{\theta}_m, \sigma_0^2 \mid \boldsymbol{\theta}, \mathbf{y}^F)$  can be sampled from the Gibbs algorithm, since the prior is conjugate. Besides, we assume the default choice of the prior of the calibration parameters  $\pi(\boldsymbol{\theta})$  to be uniform over the parameter space. The posterior distribution  $p(\boldsymbol{\theta} \mid \mathbf{y}^F, \boldsymbol{\theta}_m, \sigma_0^2)$  can be sampled from the Metropolis algorithm. The posterior distributions, MCMC algorithm and computing predictions from the posterior samples will be discussed in Appendix.

Here we show one example studied in Bayarri et al. (2007b), where data are observed from unknown reality:  $y^F(x) = 3.5 \exp(-1.7x) + 1.5 + \epsilon$ , where  $\epsilon \sim \mathcal{N}(0, 0.3^2)$ . 30 observations are available from 10 observable inputs in the domain  $x_i \in [0, 3]$ , for  $i = 1, 2, \dots, 10$ , each containing 3 replications. The computer model is  $f^M(x, \theta) = 5 \exp(-\theta x)$  with  $\theta \in [0, 50]$ . The goal is to estimate the calibration parameters and predict the unknown reality ( $3.5 \exp(-1.7x) + 1.5$ ) at  $x \in [0, 5]$ .

We use the exact observable inputs and observations given in Bayarri et al. (2007b) generated by the code below.

```
R> input=c(.110, .432, .754, 1.077, 1.399, 1.721, 2.043, 2.366, 2.688, 3.010)
R> n=length(input)
R> k=3
R> output=t(matrix(c(4.730, 4.720, 4.234, 3.177, 2.966, 3.653, 1.970, 2.267, 2.084, 2.079,
+ 2.409, 2.371, 1.908, 1.665, 1.685, 1.773, 1.603, 1.922, 1.370, 1.661,
+ 1.757, 1.868, 1.505, 1.638, 1.390, 1.275, 1.679, 1.461, 1.157, 1.530), k, n))
R> Bayarri_07<-function(x, theta){
+ 5*exp(-x*theta)
```

```
+ }
R> theta_range=matrix(c(0,50),1,2)
```

Here the mathematical model has a closed form expression so we input it as a function called Bayarri\_07. The parameter range of calibration parameter  $\theta$  is given by a vector called theta\_range. Here the mathematical model has a closed-form expression. We will discuss calibrating computer models written as differential equations in the next example.

Calibrating a mathematical model by the no-discrepancy calibration can be implemented by the code below.

```
R> set.seed(1)
R> X=matrix(1,n,1)
R> m_no_discrepancy=rcalibration(input, output,math_model = Bayarri_07,
+                               theta_range = theta_range, X =X,
+                               have_trend = T,discrepancy_type = 'no-discrepancy')
R> m_no_discrepancy
type of discrepancy function: no-discrepancy
number of after burn-in posterior: 8000
0.1385 of proposed calibration parameters are accepted
median and 95% posterior credible interval of calibration parameter 1 are
2.951997 2.264356 3.930725
```

Here we give a constant mean basis using the trend argument  $X$ , such that the mathematical model is  $f^M(x, \theta) + \mu$ . We draw 10,000 posterior samples with the first 2,000 as burn-in samples. One can adjust the number of posterior samples by argument  $S$  and  $S_0$  in the calibration function. The median of the posterior samples of  $\theta$  is 2.95, and the 95% posterior interval interval is around (2.26, 3.93). Around 14% samples was accepted by the Metropolis algorithm. To use a proposal distribution of the calibration parameter with a smaller standard deviation, one can adjust  $sd\_proposal$  below

```
R> m_no_discrepancy_small_sd=rcalibration(input, output,math_model = Bayarri_07,
+                                       theta_range = theta_range,
+                                       sd_proposal = c(rep(0.025,dim(theta_range)[1]),
+                                       rep(0.25,dim(as.matrix(input) ) [2]),0.25),
+                                       X =X, have_trend = T,discrepancy_type = 'no-discrepancy')
R> m_no_discrepancy_small_sd
type of discrepancy function: no-discrepancy
number of after burn-in posterior: 8000
0.2613 of proposed calibration parameters are accepted
median and 95% posterior credible interval of calibration parameter 1 are
2.935007 2.19352 3.933492
```

Here the first  $p_\theta$  terms in  $sd\_proposal$  is the standard deviation of the proposal distribution of the calibration parameter, chosen as 0.025 of the range of the calibration parameter. The default choice is 0.05. The next  $p_x + 1$  parameters are standard deviation of the inverse logarithm of the range parameter and nugget parameters in GaSP and S-GaSP calibration, discussed in following subsections. The median and 95% posterior credible interval with different proposal distributions do not change much in the no-discrepancy calibration in this example.

The following code gives predictions of the reality using the calibrated computer model and estimated mean with a constant mean basis by argument  $X\_testing$ . We make predictions on 200 test inputs equally spaced at  $x \in [0, 5]$ . We also compute the 95% predictive interval by argument  $interval\_est$ .

```
R> testing_input=seq(0,5,5/199)
R> X_testing=matrix(1,length(testing_input),1)
R> m_no_discrepancy_pred=predict(m_no_discrepancy,testing_input,math_model=Bayarri_07,
+                               interval_est=c(0.025, 0.975),X_testing=X_testing)
```

Posterior samples of the calibration parameter  $\theta$  and the mean parameter  $\theta_m$  in the no-discrepancy calibration are graphed by as the red rectangles in the right panel in Figure 2. The predictive mean and 95% predictive interval are graphed as the red curve and grade shaded area in the left panel, respectively. Compared to models with an estimated discrepancy function, the posterior samples from the no-discrepancy calibration are more concentrated, and the average length of 95% predictive interval is shorter. However, a large proportion of reality at  $x \in [0, 1.5]$  is not covered by the 95% posterior credible interval, due to large discrepancy between the mathematical model and reality in this domain. Next we introduce two models of discrepancy to solve this problem.

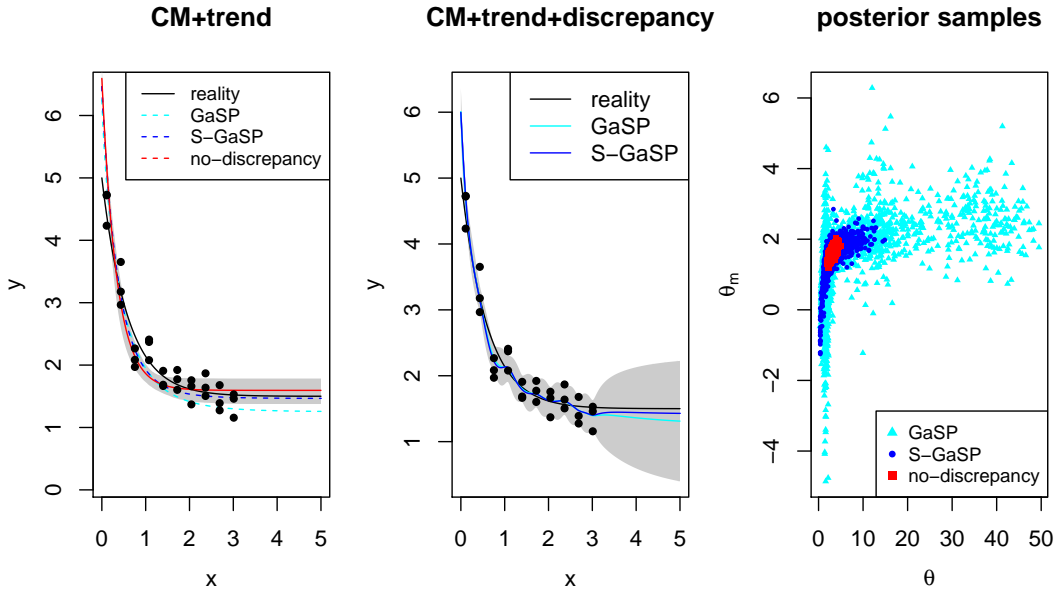


**Figure 2:** Predictions and posterior samples by the **RobustCalibration** package for the example introduced in Bayarri et al. (2007b). In the left and middle panels, The unknown reality is graphed as black curves, and field observations that contain with 3 replicates at each observable input are plotted as black circles. In the left panel, predictions of reality based on calibrated computer model (including the estimated trend parameter) by GaSP, S-GaSP and no-discrepancy calibration are graph as light blue, blue and red curves, respectively. ‘CM’ in the tile denotes the computer model and the shaded area is the 95% posterior predictive interval by the no-discrepancy calibration. In the middle panel, predictions based on the calibrated computer model, discrepancy and trend by GaSP and S-GaSP are graphed as lightblue and blue curves, respectively. The shaded area is the the 95% posterior predictive interval by the GaSP calibration. After burn-in posterior samples of calibration parameter  $\theta$  and mean parameter  $\theta_m$  by these three models are plotted in the right panel.

### Gaussian stochastic process model of discrepancy function

Assume the discrepancy function is modeled as a GaSP, meaning that for any  $\{\mathbf{x}_1, \dots, \mathbf{x}_n\}$ , the marginal distribution of discrepancy function follows a multivariate normal distribution:

$$(\delta(\mathbf{x}_1), \dots, \delta(\mathbf{x}_n))^T \mid \boldsymbol{\mu}, \sigma^2, \mathbf{R} \sim \mathcal{MN}(\boldsymbol{\mu}, \sigma^2 \mathbf{R}),$$

where  $\boldsymbol{\mu} = (\mu(\mathbf{x}_1), \dots, \mu(\mathbf{x}_n))^T$  is a vector of the mean (or trend),  $\sigma^2$  is a variance parameter, and  $\mathbf{R}$  is the correlation matrix between outputs.

Similar to the no-discrepancy calibration, we allow user to model the trend as  $\mu(\mathbf{x}_i) = h(\mathbf{x}_i)\boldsymbol{\theta}_m = \sum_{t=1}^q h_t(\mathbf{x}_i)\theta_{m,t}$ , where  $h(\mathbf{x}_i)$  is a row vector of mean basis and  $\boldsymbol{\theta}_m$  is a vector of trend parameters. Since the trend is often modeled in the computer model, the default value of the trend parameters is  $\mathbf{0}$ .

The  $(i, j)$ th element of the correlation matrix is modeled by a kernel function  $R_{i,j} = K(\mathbf{x}_i, \mathbf{x}_j)$ . We implement the separable kernel  $K(\mathbf{x}_i, \mathbf{x}_j) = \prod_{l=1}^{p_x} K_l(\mathbf{x}_i, \mathbf{x}_j)$ , where  $K_l$  models the correlation between the  $l$ th coordinate of the observable input, for  $l = 1, \dots, p_x$ . Some frequently used kernel functions are listed in Table 1. The range parameters  $\gamma$  are estimated by default.

Denote the nugget parameter by the noise variance to signal variance ratio  $\eta = \sigma_0^2/\sigma^2$ . Marginalizing out discrepancy  $\delta$ , one has  $\mathbf{y}^F \sim \mathcal{MN}(\mathbf{f}_\theta^M + \mathbf{H}\boldsymbol{\theta}_m, \sigma_0^2 \tilde{\mathbf{R}})$ , where  $\tilde{\mathbf{R}} = \mathbf{R}/\eta + \mathbf{\Lambda}$ . Here by default  $\mathbf{\Lambda} = \mathbf{I}_n$ , and we allow users to specify the inverse diagonal terms of  $\mathbf{\Lambda}$  by the weights argument:  $w_i = 1/\Lambda_{ii}$ , for  $i = 1, \dots, n$ .

The MLE of the trend and noise variance parameters in the GaSP calibration follows  $\hat{\boldsymbol{\theta}}_m = (\mathbf{H}^T \tilde{\mathbf{R}}^{-1} \mathbf{H})^{-1} \mathbf{H}^T \tilde{\mathbf{R}}^{-1} (\mathbf{y} - \mathbf{f}_\theta^M)$  and  $\hat{\sigma}_0^2 = S_K^2/n$ , where  $S_K^2 = (\mathbf{y} - \mathbf{f}_\theta^M - \mathbf{H}^T \hat{\boldsymbol{\theta}}_m)^T \tilde{\mathbf{R}}^{-1} (\mathbf{y} - \mathbf{f}_\theta^M - \mathbf{H}^T \hat{\boldsymbol{\theta}}_m)$ . Plugging the MLE of trend and noise variance parameters, one can numerically maximize the profile

GaSP calibration	Product kernel ( $K(\mathbf{d}) = \prod_{l=1}^{p_x} K_l(d_l)$ )
Matérn $\alpha = 5/2$	$K_l(d_l) = \left(1 + \frac{\sqrt{5}d_l}{\gamma_l} + \frac{5d_l^2}{3\gamma_l^2}\right) \exp\left(-\frac{\sqrt{5}d_l}{\gamma_l}\right)$
Matérn $\alpha = 3/2$	$K_l(d_l) = \left(1 + \frac{\sqrt{3}d_l}{\gamma_l}\right) \exp\left(-\frac{\sqrt{3}d_l}{\gamma_l}\right)$
Power exponential	$K_l(d_l) = \exp\left\{-\left(\frac{d_l}{\gamma_l}\right)^{\alpha_l}\right\}, 0 < \alpha_l \leq 2$
S-GaSP calibration	Scaled kernel ( $K_{Z_d}(\mathbf{x}_a, \mathbf{x}_b) = K(\mathbf{x}_a, \mathbf{x}_b) - \mathbf{r}^T(\mathbf{x}_a)\mathbf{R}_z^{-1}\mathbf{r}(\mathbf{x}_b)$ )

**Table 1:** Correlation functions currently implemented in **RobustCalibration**. For any  $\mathbf{x}_a, \mathbf{x}_b \in \mathcal{X}$ , denote  $\mathbf{d} = \mathbf{x}_a - \mathbf{x}_b = (d_1, \dots, d_{p_x})^T$ . For any kernel  $K$ , the discretized scaled kernel  $K_{Z_d}(\mathbf{x}_a, \mathbf{x}_b)$  with discretization points on observed points  $\mathbf{x}_1, \dots, \mathbf{x}_n$  was implemented in the S-GaSP calibration, where  $\mathbf{R}_z := \mathbf{R} + n\mathbf{I}_n/\lambda_z$ , and  $\mathbf{r}(\mathbf{x}) = (K(\mathbf{x}, \mathbf{x}_1), \dots, K(\mathbf{x}, \mathbf{x}_n))^T$  for any  $\mathbf{x}$ .

likelihood to obtain the calibration, kernel and nugget parameters in GaSP calibration:

$$(\hat{\boldsymbol{\theta}}, \hat{\gamma}, \hat{\eta}) = \underset{(\boldsymbol{\theta}, \gamma, \eta)}{\operatorname{argmax}} \mathcal{L}_K(\boldsymbol{\theta}, \gamma, \eta, | \hat{\boldsymbol{\theta}}_m, \hat{\sigma}_0^2) \quad (4)$$

where the profile likelihood  $\mathcal{L}_K(\boldsymbol{\theta}, \gamma, \eta, | \hat{\boldsymbol{\theta}}_m, \hat{\sigma}_0^2)$  with kernel  $K(\cdot, \cdot)$  has a closed form expression, given in the Appendix.

After obtaining the estimation of the parameters, the predictive distribution of reality on any  $\mathbf{x}^*$  can be obtained by plugging the estimator

$$y^R(\mathbf{x}^*) | \mathbf{y}^F, \hat{\boldsymbol{\theta}}_m, \hat{\sigma}_0^2, \hat{\boldsymbol{\theta}}, \hat{\gamma}, \hat{\eta} \sim \mathcal{N}(\hat{\mu}(\mathbf{x}^*), \hat{\sigma}_0^2(K^*/\hat{\eta} + \Lambda^*)), \quad (5)$$

where  $\Lambda^*$  is the weight at  $\mathbf{x}^*$  that is set to be 1 by default, and

$$\begin{aligned} \hat{\mu}(\mathbf{x}^*) &= f^M(\mathbf{x}^*, \hat{\boldsymbol{\theta}}) + \mathbf{h}(\mathbf{x}^*)\hat{\boldsymbol{\theta}}_m + \mathbf{r}^T(\mathbf{x}^*)\tilde{\mathbf{R}}^{-1}(\mathbf{y}^F - \mathbf{f}(\mathbf{x}_{1:n}, \hat{\boldsymbol{\theta}}) - \mathbf{H}\hat{\boldsymbol{\theta}}_m), \\ K^* &= K(\mathbf{x}^*, \mathbf{x}^*) - \mathbf{r}^T(\mathbf{x}^*)\tilde{\mathbf{R}}^{-1}\mathbf{r}(\mathbf{x}^*), \end{aligned}$$

with  $\mathbf{r}(\mathbf{x}^*) = (K(\mathbf{x}^*, \mathbf{x}_1), \dots, K(\mathbf{x}^*, \mathbf{x}_n))^T$ . Noting that the calibrated computer model  $f^M(\mathbf{x}^*, \hat{\boldsymbol{\theta}})$  is of interest for predicting the reality, due to its interpretability. Thus, we recorded three slots for predicting the reality: 1) `math_model_mean_no_trend` ( $f^M(\mathbf{x}^*, \hat{\boldsymbol{\theta}})$ ), 2) `math_model_mean` ( $f^M(\mathbf{x}^*, \hat{\boldsymbol{\theta}}) + \mathbf{h}(\mathbf{x}^*)\hat{\boldsymbol{\theta}}_m$ ), and 3) `mean` ( $\hat{\mu}(\mathbf{x}^*)$ ). Furthermore, users can also output the predictive interval from the predictive distribution in (5) by letting argument `interval_est=T` and specifying `interval_est=c(0.025, 0.975)` in the `predict.rcalibration` function. For example, setting `interval_est=c(0.025, 0.975)` in the `predict.rcalibration` function gives the 95% predictive interval of the reality. Furthermore, if `interval_data=T`, the predictive interval of the data will be computed.

Numerically computing MLE here can be unstable as the profile likelihood  $\mathcal{L}_K(\boldsymbol{\theta}, \gamma, \eta | \hat{\boldsymbol{\theta}}_m, \hat{\sigma}_0^2)$  can be highly nonlinear and nonconvex with respect to the parameters  $(\boldsymbol{\theta}, \gamma, \eta)$ . To obtain the uncertainty assessment of parameter estimation and avoid instability in numerical search of MLE, we implement the MCMC algorithm for Bayesian inference. The posterior distribution is

$$p(\boldsymbol{\theta}_m, \sigma_0^2, \boldsymbol{\theta}, \gamma, \eta | \mathbf{y}^F) \propto p_K(\mathbf{y}^F | \boldsymbol{\theta}, \gamma, \eta, \boldsymbol{\theta}_m, \sigma_0^2) \pi(\boldsymbol{\theta}) \pi(\boldsymbol{\theta}_m, \sigma_0^2, \gamma, \eta), \quad (6)$$

where  $p_K(\cdot)$  is the multivariate normal density with covariance function of the discrepancy being  $\sigma^2 K(\cdot, \cdot)$ , and  $\pi(\boldsymbol{\theta})$  is the prior of the calibration parameters, assumed to be uniform over the parameter space. The prior of the mean, variance, kernel and nugget parameters takes the form below

$$\pi(\boldsymbol{\theta}_m, \sigma_0^2, \gamma, \eta) \propto \frac{\pi(\gamma, \eta)}{\sigma_0^2},$$

where the usual reference prior of the trend and variance parameters  $\pi(\boldsymbol{\theta}_m, \sigma_0^2) \propto 1/\sigma_0^2$  is assumed. We use jointly robust prior as the prior for the kernel and nugget parameters  $\pi(\gamma, \eta)$ , as it has a similar tail density decay rate as the reference prior, but it is easier and more robust to compute (Gu, 2018). Closed form expressions of the posterior distributions and MCMC algorithm are provided in Appendix.

In **RobustCalibration**, we record the posterior samples after burn-in  $(\boldsymbol{\theta}_m^{(i)}, (\sigma_0^{(i)})^2, \boldsymbol{\theta}^{(i)}, \gamma^{(i)}, \eta^{(i)})$  for  $i = S_0 + 1, \dots, S$ . Users can also record a subset of posterior samples for storage reasons by thinning the Markov chain. For instance, if 1/5 of the posterior samples shall be recorded, users can set `thinning=5` in the `rcalibration` function.

Similar to the predictions based on MLE, we also output three types of predictions. For instance,

	RMSE (CM+trend)	RMSE (with discrepancy)	$P_{CI}(95\%)$	$L_{CI}(95\%)$
GaSP	0.253	0.151	0.975	0.884
S-GaSP	0.224	0.138	0.955	1.15
No-discrepancy	0.250	/	0.795	0.409

**Table 2:** Predictive accuracy and uncertainty assessment. The RMSE of the out-of-sample prediction based on the calibrated computer model (CM) and trend are shown in the second column. The predictive RMSE by the summation of the calibrated computer model, trend and discrepancy are given in the third column. The proportion of the held-out reality covered in the 95% predictive interval, and average lengths of predictive intervals are given in the last two columns, respectively.

suppose we obtain  $S$  posterior samples with first  $S_0$  samples used as burn-in samples, the predictive mean of the reality can be computed by

$$\hat{\mu}(\mathbf{x}^*) = \sum_{i=S_0+1}^S f^M(\mathbf{x}^*, \boldsymbol{\theta}^{(i)}) + \mathbf{h}(\mathbf{x}^*)\boldsymbol{\theta}_m^{(i)} + (\mathbf{r}^{(i)}(\mathbf{x}^*))^T (\tilde{\mathbf{R}}^{(i)})^{-1} (\mathbf{y}^F - \mathbf{f}^M(\mathbf{x}_{1:n}, \boldsymbol{\theta}^{(i)}) - \mathbf{H}\boldsymbol{\theta}_m^{(i)})$$

where  $\mathbf{r}^{(i)}(\mathbf{x}^*)$  and  $\tilde{\mathbf{R}}^{(i)}$  are obtained by plugging in the  $i$ th posterior samples. The predictive interval can also be computed by specifying the argument `interval_est` in `predict.rcalibration` function.

Code below implements the GaSP calibration of parameter estimation and predictions for the example in (Bayarri et al., 2007b) that was discussed in the previous subsection.

```
R> m_gasp=rcalibration(input, output, math_model = Bayarri_07, theta_range = theta_range,
+ X =X, have_trend = T, discrepancy_type = 'GaSP')
R> m_gasp_pred=predict(m_gasp, testing_input, math_model=Bayarri_07,
+ interval_est=c(0.025, 0.975), X_testing=X_testing)
```

Predictions and posterior samples from the GaSP calibration are graphed in Figure 2. The associated predictive error is shown in Table 2. Comparing the first two rows in Table 2, the predictive RMSE in the no-discrepancy calibration is around 0.25, and it decreases to 0.15, after adding the discrepancy function modeled by GaSP. Around 97.5% of the held-out truth is covered by the 95% credible interval of the reality in GaSP calibration, indicating accurate uncertainty assessment of the prediction in this example. In comparison, the 95% credible interval of the reality in no-discrepancy calibration only covers around 80% of the held-out reality.

As shown in the right panel in 2, the posterior samples from GaSP spread over a larger parameter range, reflecting larger uncertainty in the parameter space. This is because the discrepancy modeled by GaSP with the frequently used kernel listed in Table 1 is very flexible. As a result, the calibrated mathematical model alone may be less accurate in predictive the reality. We discuss a recent approach that induces a scaled kernel to constrain the discrepancy function in the next subsection.

### Calibration by scaled Gaussian stochastic process model of discrepancy

Scaling the kernel of GaSP for model calibration was introduced in Gu and Wang (2018), where the random  $L_2$  distance between the discrepancy model was scaled to have more prior probability mass at small values, as small distance indicates the computer model fits the reality well. Note that we leave  $\sigma^2$  as a free parameter estimated by data, and thus S-GaSP is a flexible model of discrepancy.

In **RobustCalibration**, we implemented the discretized S-GaSP to scale the random mean squared error between the reality and computer model:

$$\delta_{z_d}(\mathbf{x}) = \left\{ \delta(\mathbf{x}) \mid \frac{1}{n} \sum_{i=1}^n \delta(\mathbf{x}_i)^2 = Z_d \right\} \quad (7)$$

with the subscript 'd' denoting discretization, and the density of  $Z_d$  is defined as

$$p_{Z_d}(z) = \frac{g_{Z_d}(z) p_\delta(Z_d = z)}{\int_0^\infty g_{Z_d}(t) p_\delta(Z_d = t) dt} \quad (8)$$

where  $p_\delta(Z_d = z)$  is the density of  $Z_d$  induced by GaSP with kernel  $K(\cdot, \cdot)$ , and  $g_{Z_d}(\cdot)$  is a nondecreasing function that places more probability mass on smaller values of the  $L_2$  loss. For a frequently used kernel function in Table 1, the probability measure  $p_\delta(Z_d = z)$  places a large probability at large  $L_2$  loss when correlation is large, dragging the calibrated computer model away from the reality. In

S-GaSP calibration, the measure for  $Z_d$  was scaled to have more probability mass near zero by a scaling function  $g_{Z_d}(z)$ . The default scaling function is assumed to be an exponential distribution,

$$g_{Z_d}(z) = \frac{\lambda_z}{2\sigma^2} \exp\left(-\frac{\lambda_z z}{2\sigma^2}\right), \quad (9)$$

where  $\lambda_z$  controls how large the scaling factor is. Large  $\lambda_z$  induces more prior probability mass concentrating at the origin. As shown in Gu et al. (2018b),  $\lambda_z \propto \sqrt{n}$  guarantees the convergence of the calibration parameters to the ones that minimize the  $L_2$  distance between the reality and computer model. Furthermore, the calibrated computer models can be far away from reality when the nugget  $\eta$  is small and the range  $\gamma$  is large (corresponding to a large correlation). Thus we let the default choice be  $\lambda_z = \sqrt{10n} \|\tilde{\gamma}\|/\eta$ , where  $\tilde{\gamma} = (\gamma_1/L_1, \dots, \gamma_{p_x}/L_{p_x})^T$ , with  $L_i$  being the length of domain of the  $i$ th coordinate of the calibration parameter. We allow users to specify the scaling parameters by the `lambda_z` in the `rcalibration` function.

The default choice of kernel scaling in (8) and (9) has computational advantages. After marginalizing out  $Z_d$ , it follows from Lemma 2.4 in Gu and Wang (2018) that  $\delta_{z_d}(\cdot)$  has the covariance function

$$\sigma^2 K_{z_d}(\mathbf{x}_a, \mathbf{x}_b) = \sigma^2 \left\{ K(\mathbf{x}_a, \mathbf{x}_b) - \mathbf{r}^T(\mathbf{x}_a) \left( \mathbf{R} + \frac{n\mathbf{I}_n}{\lambda_z} \right)^{-1} \mathbf{r}(\mathbf{x}_b) \right\} \quad (10)$$

for any  $\mathbf{x}_a, \mathbf{x}_b$ , where  $\mathbf{r}(\mathbf{x}) = (K(\mathbf{x}, \mathbf{x}_1), \dots, K(\mathbf{x}, \mathbf{x}_n))^T$  for any  $\mathbf{x}$ . The covariance matrix of the S-GaSP model of  $(\delta_z(\mathbf{x}_1), \dots, \delta_z(\mathbf{x}_n))^T$  follows

$$\sigma^2 \mathbf{R}_z = \sigma^2 \left\{ \mathbf{R} - \mathbf{R} \left( \mathbf{R} + \frac{n\mathbf{I}_n}{\lambda_z} \right)^{-1} \mathbf{R} \right\}. \quad (11)$$

The closed-form expression in Equ. (10) avoids sampling  $(\delta_z(\mathbf{x}_1), \dots, \delta_z(\mathbf{x}_n))$  to obtain  $Z_d$  from the posterior distribution, which greatly improves the computational speed.

For any covariance function  $K(\cdot, \cdot)$  in GaSP calibration, a scaled kernel was induced in S-GaSP calibration, shown in the last row of Table 1. The S-GaSP model of the discrepancy can be specified by the argument `discrepancy_type='S-GaSP'` in the `rcalibration` function. Similar to the model of GaSP-calibration, we also provide MLE and posterior samples for estimating the parameters, with argument `method='mle'` and `method='post_sample'`, respectively. The MLE of parameters in S-GaSP are computed by maximizing the profile likelihood

$$(\hat{\theta}, \hat{\gamma}, \hat{\eta}) = \underset{(\theta, \gamma, \eta)}{\operatorname{argmax}} \mathcal{L}_{K_{Z_d}}(\theta, \gamma, \eta, | \hat{\theta}_m, \hat{\sigma}_0^2) \quad (12)$$

where  $(\hat{\theta}_m, \hat{\sigma}_0^2)$  denotes the MLE of trend and noise variance parameters in S-GaSP calibration, and  $\mathcal{L}_{K_{Z_d}}$  is the profile likelihood with respect to scaled kernel  $K_{Z_d}$  in (10) of modeling the discrepancy. Here one can simply replace the kernel  $K$  from GaSP calibration to kernel  $K_{Z_d}$  from S-GaSP calibration. Furthermore, predictions and intervals can be obtained by `predict.rcalibration` function as well.

We provide the code that implements S-GaSP calibration and prediction of the example in Bayarri et al. (2007b) below.

```
R> m_sgasp=rcalibration(input, output,math_model = Bayarri_07,theta_range = theta_range,
+                      X=X, have_trend = T,discrepancy_type = 'S-GaSP')
R> m_sgasp_pred=predict(m_sgasp,testing_input,math_model=Bayarri_07,
+                      interval_est=c(0.025, 0.975),X_testing=X_testing)
```

Predictions from S-GaSP are graphed as blue curves in Figure 2 and numerical comparisons are given in Table 2. With an estimated discrepancy by S-GaSP, the prediction of reality is more accurate at  $x \in [0.5, 1.5]$ , compared to no-discrepancy calibration. Note that the prediction by the S-GaSP model also extrapolates the reality at  $x \in [3, 5]$  accurately, because the calibrated computer model is closer to the truth. Furthermore, the 95% posterior credible interval by S-GaSP covers around 95% of the held-out samples.

### Calibration with repeated experiments

Repeated experiments or replicates are commonly used in experiments to validate a scientific finding, or to reproduce experimental outcomes. Obtaining a set of replicates of the same experiment is helpful to reduce the experimental error. Consider, for example,  $k_i$  replicates are available for each observable input  $\mathbf{x}_i$ , denoted as  $\mathbf{y}_i^F = (y_1^F(\mathbf{x}_i), \dots, y_{k_i}^F(\mathbf{x}_i))^T$ . Denote  $\tilde{\mathbf{y}}^F = (\sum_{j=1}^{k_1} y_j^F(\mathbf{x}_1)/k_1, \dots, \sum_{j=1}^{k_n} y_j^F(\mathbf{x}_n)/k_n)^T$  the

aggregated data. The probability density of the field observations can be written as

$$\begin{aligned} p(\mathbf{y}_1^F, \dots, \mathbf{y}_n^F \mid \boldsymbol{\mu}, \delta, \boldsymbol{\theta}, \sigma_0^2) &= (2\pi\sigma_0^2)^{-\frac{\sum_{i=1}^n k_i}{2}} \exp\left(-\frac{\sum_{i=1}^n \omega_i \sum_{j=1}^{k_i} (y_j^F(\mathbf{x}_i) - f^M(\mathbf{x}_i, \boldsymbol{\theta}) - \mu_i - \delta(\mathbf{x}_i))^2}{2\sigma_0^2}\right) \\ &= (2\pi\sigma_0^2)^{-\frac{\sum_{i=1}^n k_i}{2}} \exp\left(-\frac{S_f^2}{2\sigma_0^2} - \frac{\sum_{i=1}^n k_i \omega_i (\bar{y}_i^F - f^M(\mathbf{x}_i, \boldsymbol{\theta}) - \mu_i - \delta(\mathbf{x}_i))^2}{2\sigma_0^2}\right) \end{aligned}$$

where  $S_f^2 = \sum_{i=1}^n \omega_i \sum_{j=1}^{k_i} (y_j^F(\mathbf{x}_i) - \bar{y}_i^F)^2 = \sum_{i=1}^n \omega_i (\mathbf{y}_i^F - \bar{y}_i^F \mathbf{1}_{k_i})^T (\mathbf{y}_i^F - \bar{y}_i^F \mathbf{1}_{k_i})$  with subscript ‘f’ denoting field observations. After integrating out the discrepancy term, assumed to be modeled as a GaSP, the marginal likelihood of the parameters follows

$$\mathcal{L}_K(\boldsymbol{\theta}, \boldsymbol{\theta}_m, \sigma_0^2, \gamma, \eta) \propto (\sigma_0^2)^{-\frac{\sum_{i=1}^n k_i}{2}} |\tilde{\mathbf{R}}|^{-\frac{1}{2}} \exp\left\{-\frac{(\bar{\mathbf{y}}^F - \mathbf{f}_\theta^M - \boldsymbol{\mu} \mathbf{1}_n)^T \tilde{\mathbf{R}}^{-1} (\bar{\mathbf{y}}^F - \mathbf{f}_\theta^M - \boldsymbol{\mu} \mathbf{1}_n)}{2\sigma_0^2} - \frac{S_f^2}{2\sigma_0^2}\right\} \quad (13)$$

where  $\tilde{\mathbf{R}} = (\mathbf{R}/\eta + \tilde{\mathbf{\Lambda}})$ , with  $\tilde{\mathbf{\Lambda}}$  being an diagonal matrix with diagonal entry  $\Lambda_{ii} = 1/(\omega_i k_i)$ , for  $i = 1, 2, \dots, n$ , and  $\eta = \sigma_0^2/\sigma^2$ . The S-GaSP calibration with replications can also be defined, by simply replacing  $\mathbf{R}$  by  $\mathbf{R}_z$  where the  $(i, j)$ th term is defined by the scaled kernel in Table 1.

The likelihood in (13) has a clear computational advantage. If one directly compute the covariance and its inversion, the computational complexity is  $O((\sum_{i=1}^n k_i)^3)$ , while the computational order by Equation (13) is only  $O(n^3) + O(\sum_{i=1}^n k_i)$ . Suppose  $k_i = k$ , for  $i = 1, \dots, n$ , using Equation (13) is around  $k^3$  times faster than directly computing the likelihood, with no loss of information.

In **RobustCalibration** package, one can specify replications by inputting a  $n \times k$  matrix into the argument observations in the `rcalibration` function for scenarios with  $n$  observable inputs, each containing  $k$  repeated measurements. Or one can give a list observations in the `rcalibration` function with size  $n$ , where each element in the list contains  $k_i$  values of replicates, for  $i = 1, \dots, n$ . For observations with replicates, MLE and posterior sampling were implemented in `rcalibration` function, and predictions were implemented in `predict.rcalibration` function.

## Statistical emulator

In **RobustCalibration** package, users can specify a mathematical model by `math_model` in `rcalibration` function, if the closed form expression of the mathematical model is available. However, closed form solutions of physical systems are typically unavailable and numerical solvers are required. Simulating the outputs from computer models can be slow. For instance, the TITAN2D computer model of simulating pyroclastic flows for geological hazard quantification takes roughly 8 minutes per set of inputs (Simakov et al., 2019). As hundreds of thousands of model runs are sometimes required for model calibration, directly computing the computer model by numerical methods is often prohibitive. In this scenario, we construct a statistical emulator as a surrogate model, to approximate the computer simulation, based on a small number of computer model runs. Gaussian stochastic process emulator has been widely used as a surrogate model for emulating computer experiments (Sacks et al., 1989).

To start with, assume we obtained the output of computer model at  $D$  input design points,  $(\boldsymbol{\theta}_1, \dots, \boldsymbol{\theta}_D)$ , often selected from an ‘‘in-fill’’ design, such as the latin hypercube design (Santner et al., 2003). There are two types of computer model outputs: 1) scalar-valued output:  $f^M(\boldsymbol{\theta}) \in \mathbb{R}$ , and 2) vectorized output at  $k$  coordinates  $\mathbf{f}^M(\mathbf{x}_{1:k}, \boldsymbol{\theta}) \in \mathbb{R}^k$ , where  $k$  can be as large as  $10^6$ . Various packages are available for fitting scalar-valued GP emulators, such as **DiceKriging** (Roustant et al. (2012)), **GPfit** (MacDonald et al. (2015)), and **RobustGaSP** (Gu et al. (2019)). Some of these packages were used in Bayesian model calibration packages (Palomo et al., 2015; Carmassi et al., 2018). However, the emulator of the vectorized output was rarely integrated for model calibration.

In **RobustCalibration**, we call the `rgasp` function and `ppgasp` function from the **RobustGaSP** package for emulating scalar-valued and vectorized computer model outputs, respectively. The parallel partial Gaussian process (PP-GaSP) by the `ppgasp` function has two advantages. First, computing the predictive mean by the PP-GaSP only takes  $O(kD^2) + O(D^3)$  operations. The linear computational order with respect to  $k$  is suitable for computer model at a massive size of coordinates. Second, the PP-GaSP emulator is typically more robust compared to other methods, as covariance over  $\boldsymbol{\theta}$  is shared across all grids. Further more, the kernel parameters are estimated by the marginal posterior mode with robust parameterization, typically avoiding the degenerated scenarios that causes poor emulation results Gu et al. (2018a). The PP-GaSP have been applied in emulating computer model with vectorized outputs at large number of coordinates, such as the TITAN2D computer model in Gu and Berger (2016), and the mechanical finite element model in Anderson et al. (2019).

To call the emulator, users can select argument `simulator=0`, and then input the simulation runs

into arguments `input_simul`, and `output_simul`. One can input a vector into `output_simul` to emulate scalar-valued computer models, or a matrix into `output_simul` to call the PP-GaSP emulator for vectorized outputs. For both scenarios, we use a modular approach of fitting PP-GaSP emulator advocated in e.g. (Bayarri et al., 2007b; Liu et al., 2009), where the predictive distribution of the emulator depends on simulator runs, but not field observations. After fitting an emulator, the predictive mean of the PP-GaSP emulator will be used to approximate the computer model at any unobserved  $\theta^*$  by default.

Here we discuss a computer model written as ordinary different equations (ODEs) from Box and Coutie (1956), where the interaction between two chemical substances  $y_1$  and  $y_2$  are modeled as

$$\begin{aligned} \dot{y}_1(t) &= 10^{\theta_1-3}y_1(t), \\ \dot{y}_2(t) &= 10^{\theta_1-3}y_1(t) - 10^{\theta_2-3}y_2(t). \end{aligned}$$

In each of the 6 time point  $t = 10, 20, 40, 80, 160$  and  $320$ , 2 replicates of the second chemical substance are available in Box and Coutie (1956). Initial conditions are  $y_1(t = 0) = 100$  and  $y_2(t = 0) = 0$ . The computer model contains two parameters  $\theta_1 \in [0.5, 1.5]$  and  $\theta_2 \in [0.5, 1.5]$ . Although this is a toy example, **RobustCalibration** package is applicable to many other ODE systems, such as epidemiological compartment models (Li and Gu, 2021) and atmospheric models (Lorenz, 1996).

We first call the default method in the `ode` function from the **deSolve** package (Soetaert et al., 2010), to numerically solve the ODEs at a given initial conditions and parameters.

```
library(deSolve)
R> Box_model <- function(time, state, parameters) {
+   par <- as.list(c(state, parameters))
+   with(par, {
+     dM1=-10^{parameters[1]-3}*M1
+     dM2=10^{parameters[1]-3}*M1-10^{parameters[2]-3}*M2
+     list(c(dM1, dM2))
+   })
+ }
R> Box_model_solved<-function(input, theta){
+   init <- c(M1 = 100 , M2 = 0)
+   out <- ode(y = init, times = c(0,input), func = Box_model, parms = theta)
+   return(out[-1,3])
+ }
```

We then input the observations from Box and Coutie (1956) and specify the range of calibration parameters below.

```
R> n=6
R> k=2
R> output=matrix(c(19.2,14,14.4,24,42.3,30.8,42.1,40.5,40.7,46.4,27.1,22.3),n,k)
R> input=c(10,20,40,80,160,320)
R> theta_range=matrix(c(0.5,0.5,1.5,1.5),2,2)
R> testing_input=as.matrix(seq(1,350,1))
```

We compare the model with the numerical solver by the **deSolve** package, and by the GaSP emulator approach below. We first implement the direct approach for model calibration and prediction, where the numerical solver is called for each posterior sample. The cost of computational time is recorded.

```
R> m_sgasp_time=system.time({
+   m_sgasp=rcalibration(input,output,math_model=Box_model_solved,
+                       sd_proposal=c(0.25,0.25,1,1),
+                       theta_range=theta_range)
+   m_sgasp_pred=predict(m_sgasp,testing_input,math_model=Box_model_solved,
+                       interval_est=c(0.025,0.975))})
```

We then generate 50 design points from maximin latin hypercube design by the **Ihs** package, and run numerical solver at these design points, for each of the test input. Note here for calibration parameter, the simulator outputs a vector  $f^M(t_{1:k}, \theta) \in \mathbb{R}^k$ . So the PP-GaSP emulator is called for emulating the output at all time points. The simulator runs are then specified as `input_simul` and `output_simul` in `rcalibration` function. We let `simul_type=0` to call the emulator instead of the numerical solver for each posterior sample. The total computational time for simulation and model calibration are recorded.

```

R> m_sgasp_emulator_time=system.time({
+   ##constructing simulation data
+   D=50
+   p=2
+   lhs_sample=maximinLHS(n=D,k=p)
+   input_simul=matrix(NA,D,p)
+   input_simul[,1]=lhs_sample[,1]+0.5
+   input_simul[,2]=lhs_sample[,2]+0.5
+   k=length(testing_input)
+
+   output_simul=matrix(NA,D,k)
+   for(i_D in 1:D){
+     output_simul[i_D,]=Box_model_solved(c(testing_input), input_simul[i_D,])
+   }
+   ##create loc_index_emulator as a subset of the simulation output
+   loc_index_emulator=rep(NA,n)
+   for(i in 1:n){
+     loc_index_emulator[i]=which(testing_input==input[i])
+   }
+
+   ##emulator
+   m_sgasp_with_emulator=rcalibration(input,output,simul_type=0,
+                                     input_simul=input_simul, output_simul=output_simul,simul_nug=T,
+                                     loc_index_emulator=loc_index_emulator,
+                                     sd_proposal=c(0.25,0.25,1,1),
+                                     theta_range=theta_range)
+   m_sgasp_with_emulator_pred=predict(m_sgasp_with_emulator, testing_input)
+ })
R> m_sgasp_time[3]/m_sgasp_emulator_time[3]
elapsed
3.82078

```

The approach with an emulator only costs around 1/4 of the computational time in this example, even though the numerical solver here is fast. For computer model that takes a few minutes or a few hours to run, the emulator approach can improve computational cost substantially, as shown in [Gu and Berger \(2016\)](#); [Anderson et al. \(2019\)](#).

Figure 3 gives predictions and posterior samples based on the numerical solver and the PP-GaSP emulator. First, the discrepancy (modeled by a S-GaSP) in both approaches looks to be very small, as predictive mean by the calibrated computer model and discrepancy function, and by the calibrated computer model along are very close to each other. Second, predictions and posterior distributions by the numerical solver and by the emulator are almost the same for this example. Typically the emulator approach is preferred, as it is much faster than numerically solving differential equations for each posterior sample.

### Calibration with multiple sources of observations

In reality, one may have observations of different types and they may come from multiple sources. For instance, satellite radar interferogram, observations from GPS stations, and tiltmeter observations are used to estimate the geological processes of volcanic eruption in [Anderson et al. \(2019\)](#). Multiple satellite interferograms are sometimes available for inference ([Agram and Simons, 2015](#)).

Bayesian model calibration using multiple sources of observations was discussed in [Gu and Anderson \(2018\)](#). For each source  $l$ ,  $l = 1, 2, \dots, k$ , let the field observations of the  $l$  th source at observable input  $\mathbf{x}$  be modeled as

$$\mathbf{y}_l^F(\mathbf{x}) = f_l^M(\mathbf{x}, \boldsymbol{\theta}) + \delta(\mathbf{x}) + \delta_l(\mathbf{x}) + \mu_l + \epsilon_l, \quad (14)$$

where  $f_l^M(\mathbf{x}, \boldsymbol{\theta})$  is the computer model for source  $l$ . The discrepancy function is denoted  $\delta(\mathbf{x})$  and the measurement bias is denoted as  $\delta_l(\mathbf{x})$ , which are the correlated noise terms. Measurement bias often appear at satellite radar interferogram, as atmospheric error could affect the quality of the image. The mean (or trend) of each data source is denoted as  $\mu_l$ , and the independent measurement noise is denoted as  $\epsilon_l$ .

In **RobustCalibration**, we allow users to integrate observations from multiple sources to calibrate computer models by the function `rcalibration_MS` and to make predictions using the function

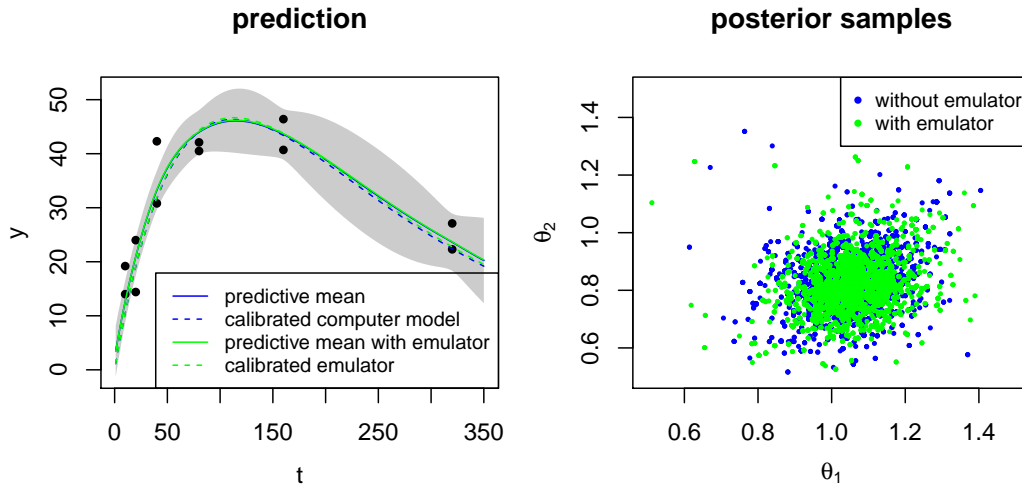


**Figure 3:** Comparison between Bayesian model calibration based on the numerical solver and the PP-GaSP emulator of the computer model. In the left panel, the green solid curve is the predictive mean by the calibrated computer model and discrepancy function, and the green dashed curves are predictions by the calibrated computer model alone, both of which call the numerical solver for each posterior sample. The same result based on the emulator is plotted as blue curves. The black dots are field observations and the shaded area is the interval 95% predictive interval of the reality by the approach that uses the PP-GaSP emulator. In the right panel, posterior samples based on the numerical solver and the PP-GaSP emulator are plotted as green dots and blue dots, respectively.

`predict_MS.rcalibration_MS`. Posterior sampling method is implemented for parameter estimation for multiple sources of data. Besides, both GaSP and S-GaSP model can be chosen to modeled the measurement bias  $\delta_l$ , for  $l = 1, \dots, k$ . Similar to calibration model with single source of data, we allow users to choose a model with no-discrepancy, and with GaSP or S-GaSP model of the discrepancy function  $\delta$ . Users can choose to have measurement bias or not. For models without measurement bias,  $\delta_l$  can be interpret as discrepancy for each source of data. Finally, we allows users to integrate different types of measurements for model calibration by inputting different designs of observable inputs.

## An overview of RobustCalibration

### Main functions

**RobustCalibration** package can be used for estimating the unobservable parameters from the computer models and for predicting the reality. Two key functions for calibrating computer models with a single type of field observations are `rcalibration` and `predict.rcalibration`. The function `rcalibration` implements the posterior sampling and MLE for parameter estimation. Additional arguments, such as handling observations from repeated experiments, choice of different discrepancy function, trend, and building a surrogate model for approximating computationally expensive computer models will be introduced next. The `rcalibration` function returns an object of the `rcalibration S4` class with posterior samples or MLE of parameters, including calibration parameters, trend parameters, noise in field observations, range and nugget parameters, to perform predictions. Then `rcalibration S4` class is used as the input in the `predict.rcalibration` function to perform predictions on a set of test inputs. The the `predict.rcalibration` function returns `predictobj.rcalibration S4` class, which contains the predictive mean of calibrated computer model, estimated trend and discrepancy function. The estimated interval at any given range can also be output by specifying a vector of the `interval_est` argument in `predict.rcalibration` function.

When observations come from from multiple sources or have different types. E.g. in calibrating geophysical model, time series of continuous GPS observations and Satellite radar interferogram (i.e. image observations) can be used jointly for estimating the unobservable physical parameters (Anderson et al., 2019). Data from multiple sources can have different observable input. In **RobustCalibration** package, we implement parameter estimation for observations from multiple sources by the `rcalibration_MS` function, which returns a `rcalibration_MS S4` class that contains posterior

samples or MLE of parameters. Then the `rcalibration_MS` class can be used as an input into the `predict_MS.rcalibration_MS` function for predicting reality.

### The rcalibration function

The `rcalibration` function is the most important function in **RobustCalibration** package, as it performs parameter estimation for data inversion. To use this function, The following arguments in the `rcalibration` function are required: 1) an  $n \times p_x$  matrix of observable inputs ( $\mathbf{x}$ ) through argument `design`, 2) field observations ( $\mathbf{y}^F$ ) by argument `observations`, 3) a  $p_\theta \times 2$  matrix of containing the lower and upper bounds of calibration parameters ( $\theta$ ) by argument `theta_range`, where each row contains the lower and upper bound of the parameter values, and 4) a mathematical model specified by `math_model` or simulation runs by `input_simul` and `output_simul` for building the emulator. The **RobustCalibration** package can handle three different kinds of field observations by argument `observations`. First, one can input a  $n$ -vector  $(y^F(x_1), \dots, y^F(x_n))^T$  into `observations`, when one field datum is available at each observable input. Second when  $k$  repeated measurements are available for each observable input, one can input an  $n \times k$  matrix of field observations, where each row contains  $k$  replicates for one observable input. Third, one can also input a list, where each element contains  $k_i$  replications at the  $i$ th observable input, for  $i = 1, \dots, n$ .

An important feature of the **RobustCalibration** package is flexible specification of the computer model. The user can specify a mathematical model by giving a function in R through the argument `math_model`, and by selecting the default choice of the simulator `simul_type=0`. The second choice is to use an emulator to approximate the computer model by choosing `simul_type=1`. Users needs to input a small set of simulation runs by `input_simul` and `output_simul` to call an emulator by the **RobustGaSP** package. Users can give an  $(p_x + p_\theta) \times D$  matrix of input and a  $D$ -vector of output into `input_simul` and `output_simul` arguments. Then the `rgasp` from **RobustGaSP** function will be called to emulate the computer model. Or `input_simul` and `output_simul` arguments can be specified as a  $(p_\theta) \times D$  matrix of input and a  $p_x \times D$  matrix of output, such that `ppgasp` function from **RobustGaSP** will be called to emulate the computer model with  $p_\theta$  dimension. To account for stochastic error or numerical approximation error in the simulator, we also allow users to specify a nugget parameter estimated by the simulator data by the argument `simul_nug=T`.

The `rcalibration` function contains many other user-specific arguments for applications in different scenarios. First, users can specify discrepancy models by GaSP and S-GaSP by the argument `discrepancy_type='GaSP'` and `discrepancy_type='S-GaSP'`, respectively. The default choice is the S-GaSP calibration. The model without a discrepancy can be specified by the argument `discrepancy_type='no-discrepancy'`. Second, for the model with or without a discrepancy function, the trend can be specified by the argument `X`. By default, the trend (or mean) of the calibration model is zero. Third, the parameter estimation approach can be specified by the `method` argument. The default choice is `method='post_sample'` where posterior samples will be drawn, and stored in the slot `post_sample` of the `rcalibration` class created by the `rcalibration` function. The MLE can be specified by the argument `method='mle'`, and the estimated parameters are stored in the slot `param_est` of `rcalibration` class. Users can change the number of MCMC samples by adjust argument `S` and `S_0` for the total number of samples and the number of burn-in samples. The standard deviation of the proposal distribution for calibration parameters, the log inverse range and log nugget parameter can be specified by the `sd_proposal` argument. Furthermore, users can thin their MCMC samples and only record a subset by the argument `thinning`. For instance, `thinning=5` means only 1/5 of the posterior samples will be recorded. Users can adjust the roughness parameter in the power exponential kernel by the argument `alpha` and choose different prior parameters in the JR prior by arguments `a` and `b`. Besides, the inverse variance of measurement error of field observations at each observable input can be taken into accounts by the `output_weights`. Finally, arguments `initial_values` and `num_initial_starts` can be specified in numerical optimization to find MLE, and they will only be useful when `method='mle'` in `rcalibration` function.

The object `rcalibration` created by the `rcalibration` function have a few key elements. First of all, if the `method='post_sample'`, the after burn-in posterior samples of parameters will be stored in the slot `post_sample`, where each row contains a posterior draw. The first  $p_\theta$  columns contains posterior samples of calibration parameters  $\theta$ . In no-discrepancy calibration, the  $p_\theta + 1$  column of `post_sample` contains posterior draws of the noise variance  $\sigma_0^2$  and the  $p_\theta + 2$  to  $p_\theta + q + 1$  columns contain the trend parameters  $\theta_m$ , if the trend ( $X$ ) is not a zero vector. In GaSP or S-GaSP calibration, the  $p_\theta + 1$  to  $p_\theta + p_x + 1$  columns record posterior draws of the log inverse range and log nugget parameters. The  $p_\theta + p_x + 2$  to  $p_\theta + p_x + q$  column record the noise variance parameter and trend parameters (if specified). The parameter  $\lambda_z$  in S-GaSP are recorded in slots `post_value` and `lambda_z`, respectively. Some diagnostic statistics, such as the location of the the accepted proposed samples are recorded in slots `accept_S`.

### The `predict.rcalibration` function

After calling the `rcalibration` function, a `rcalibration S4` class will be created. The function `rcalibration` can be used as an input into the `predict.rcalibration` function for predicting the reality on a specified matrix of test input using the argument `testing_input`. Besides, if the trend basis argument  $X$  in `rcalibration` function was previously specified, we request the users to specify the trend basis of reality at test inputs by the argument `X_testing` in function `predict.rcalibration`. If the emulator was not built, users also need to specify the mathematical model by argument `math_model`. Finally, the predictive interval can be specified by the argument `interval_est`. For instance, the 95% predictive interval can be obtained by the `interval_est=c(0.025,0.975)` argument. The interval of the field data that includes the estimated noise of field observations will be computed, if `interval_data=T`. Otherwise, the predictive interval of the reality will be computed. Finally, if the size of the noises in field data was specified by the `output_weights`, the users can also specify the variance of test data by `testing_output_weights`, which affects the predictive interval of test data.

After calling `predict.rcalibration` function, an object `predictobj.rcalibration` will be created that contains three different predictors for reality. The slot `math_model_mean_no_trend` gives the predictive mean based on calibrated computer model ( $f^M$ ). The slot `math_model_mean` gives the predictive mean based on the calibrated computer model and estimated trend ( $f^M + \mu$ ), if trend basis functions at observable input and test input are specified through  $X$  and `X_testing` in `rcalibration` and `rcalibration.predict`, respectively. The slot `mean` give the predictive mean based on calibrated computer model, estimated trend and discrepancy ( $f^M + \mu + \delta$ ). The predictive mean is typically more accurate for predicting the reality than using the computer model alone. Furthermore, if predictive interval at the specified values of the argument `interval_est` can be computed for uncertainty assessment of predictions.

### The `rcalibration_MS` function and the `predict_MS.rcalibration_MS` function

Model calibration and predictions using multiple sources of data or different types of data are implemented by `rcalibration_MS` and `rcalibration_MS.predict_MS` functions, respectively. One only need to specify 3 components: `design`, `observations`, `theta_range` and a form of mathematical model. Suppose we have a data set from  $k$  sources of observations. The `design` is a list of  $k$  elements, where each element is a matrix of observable input for each source (or each type) of observations. The argument `observations` takes a list of field observations, where each element is a vector of field observations for each source. In principle, one can have different number of observations from each source and the type may not be the same. The argument `theta_range` is a  $p_\theta \times 2$  matrix of the range of parameters, where each row  $i$  contain the minimum and maximum values of the  $i$ th coordinate of calibration parameter  $\theta$ . Furthermore, if closed form expression of mathematical models are available for each source of data, users can input a list of functions into the `math_model`. We also allow users to emulate the expensive simulation. In this scenario, one need to let `simul_type` be a vector of 1s, indicating emulators will be called for each computer model. One then needs to specify a list of `input_simul` and `output_simul` as input and output of computer simulation. In future version, we will allow users to build one emulator if the computer model is shared across all sources of data.

Users can specify various arguments in `rcalibration_MS`. For instance, the argument `index_theta` takes a list of indices for the associated calibration parameter for each computer model. For instance, suppose we have  $\theta = (\theta_1, \theta_2, \theta_3)$ , and the computer model for first source of data is related to the first two calibration parameters and the computer model for second source of data is related to second two calibration parameters. Then `index_theta` is a list where `index_theta[[1]]=c(1,2)`, and `index_theta[[2]]=c(2,3)`. Furthermore, the `measurement_bias` is a bool value to include a measurement bias or not. If `measurement_bias=T`, then equation (14) is needed and the observable for  $\delta$  is given in the `shared_design` argument. If `measurement_bias=T`, then  $\delta = 0$  and each  $\delta_i$  is the discrepancy for computer model for source  $i$ , for  $i = 1, \dots, k$ . Similar to model calibration with single source of data,, one can specify the type of discrepancy and kernel function of the discrepancy by `discrepancy_type` and `kernel_type`. Other arguments in `rcalibration_MS` are similar to `rcalibration`. After calling `rcalibration_MS`, an S4 class `rcalibration_MS` will be built, and used as an input to `predict_MS.rcalibration_MS` for making predictions.

### Additional Example

We include one additional toy example of the Lorenz-96 system used in modeling atmospheric dynamics (Lorenz, 1996). The mathematical model is written as ODEs below:

$$\dot{x}_j(t) = (x_{j+1}(t) - x_{j-2}(t))x_{j-1}(t) - x_j(t) + \theta, \quad (15)$$

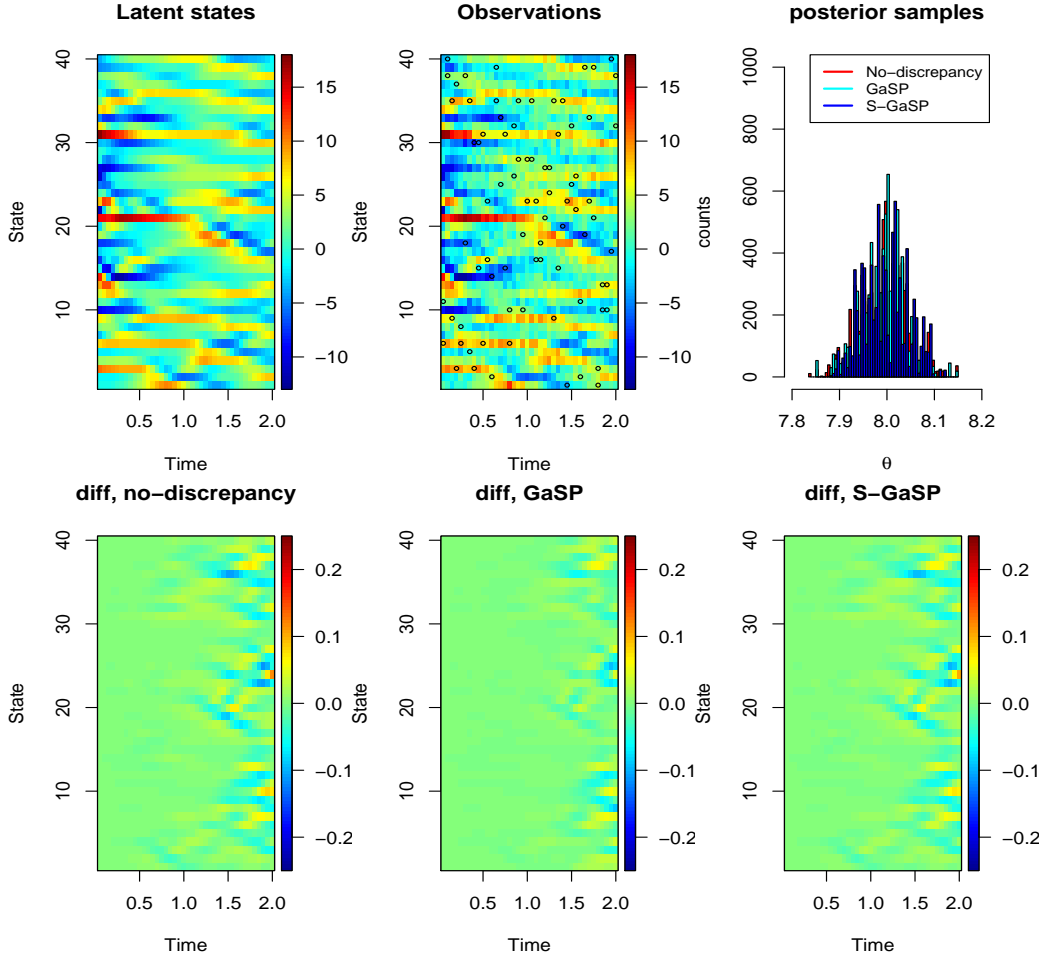


**Figure 4:** The reality and full observations of Lorenz-96 system for scenario 1 no discrepancy (Scenario 1) are plotted at the upper left panel and upper middle panel, respectively, where the black circles are the 5% observations used for model calibration. Posterior samples of calibration parameters of different calibration methods are plotted at the upper right pane. The lower panels give the difference between the reality and calibrated computer model of all latent states.

for  $j = 1, \dots, k$  states, with  $k = 40$  and  $\theta$  is a scalar value of the force. Further assume that  $x_{-1} = x_{k-1}$ ,  $x_0 = x_k$  and  $x_{k+1} = x_1$  for any  $t$ . The latent variables  $x_i$  can model the atmospheric quantities, such as temperature or pressure, measured at  $k$  positions along a constant latitude circle. This model is widely used for data assimilation (Macleam and Spiller, 2020; Brajard et al., 2020).

We consider model calibration at two scenario:

Scenario 1: 
$$y_j(t) = x_j(t) + \epsilon, \tag{16}$$

Scenario 2: 
$$y_j(t) = x_j(t) + 2t \sin\left(\frac{2\pi l}{k}\right) + \epsilon, \tag{17}$$

for  $l = 1, \dots, k$ . where  $\epsilon \sim N(0,1)$  is an independent Gaussian noise. In the first scenario the mathematical model is a true model and in the second scenario, a discrepancy term is included for simulating the field data. The discrepancy is treated unknown. We initialize the states by a multivariate normal with the covariance generated from a Wishart distribution with  $k$  degrees of freedom and a diagonal scale matrix. We use the Runge Kutta method with order 4 to numerically solve the systems. Since the computer model is fast so we do not include an emulator. We simulate the reality on 40 time points, with time step 0.05 between them.

The unobserved reality simulated by the Lorenz-96 system is plotted in upper model panel in Figure 4. Only 5% observations (i.e. 2 observations at each time point, graphed as black circles in upper middle panel) are available for model calibration. The posterior parameters of no-discrepancy calibration, GaSP and S-GaSP calibration are graphed in the upper right panels. Note that here since the computer model (Lorenz-96) is the true model, the no-discrepancy calibration is expected to

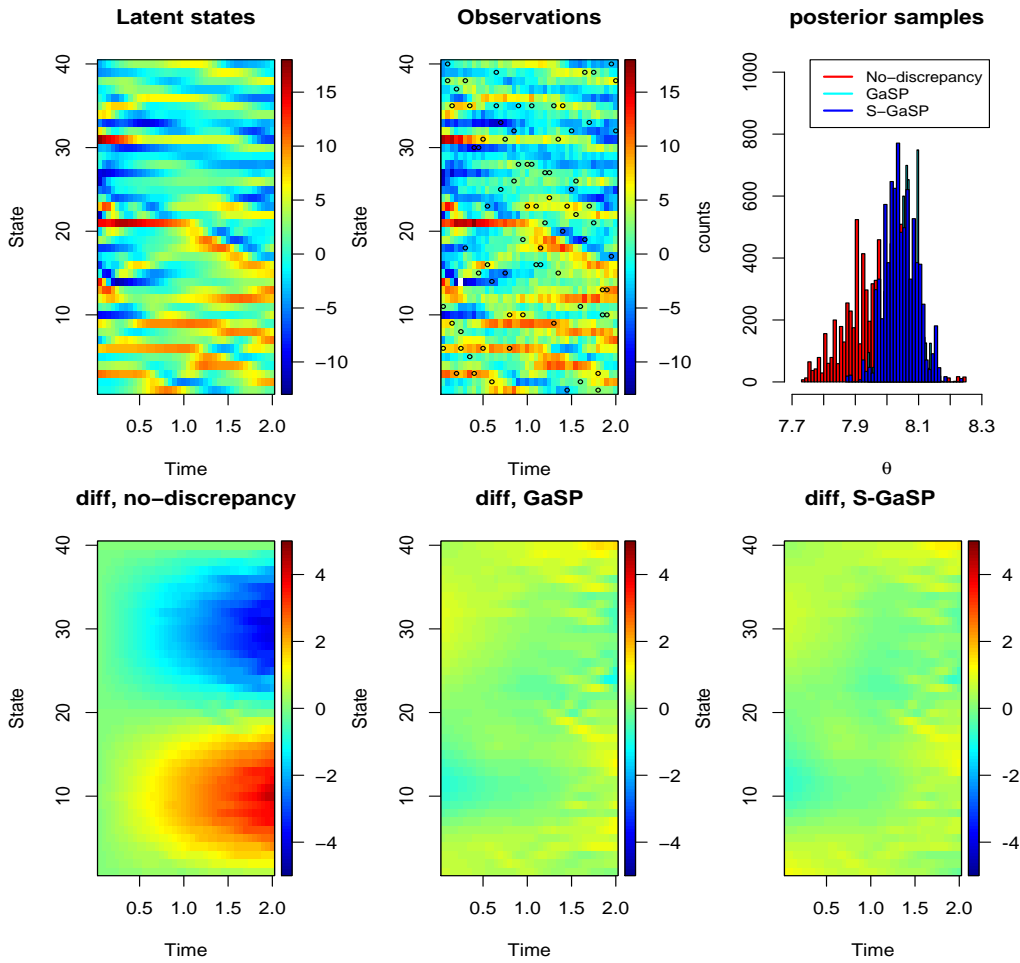


**Figure 5:** The reality of a discrepancy-included Lorenz-96 system (Scenario 2) is plotted at the upper left panel, The simulated observations are graphed at the upper middle panel, where the 5% of the observations plotted as black circles are used in model calibration. Posterior samples of calibration parameters of different calibration methods are plotted at the upper right panel. The lower panels give the difference between the reality and calibrated computer model with discrepancy (if estimated) of all latent states.

perform well. Even though one allows a flexible discrepancy function, modeled as GaSP or S-GaSP, it seems parameters are estimated reasonably well in both approach. In all methods, posterior samples are centered around the true parameter ( $\theta = 8$ ), and the range of posterior samples is short compared to the parameter range  $[-20, 20]^2$ . The estimate states by the calibrated computer model and the reality are plotted in the lower panels in Figure 4. All methods have small estimation errors, as the parameters are estimated well.

The reality, observations, posterior samples and predictions from different calibration models for a discrepancy-included Lorenz-96 system are graphed in Figure 5. Note that since the discrepancy is included, there is no true calibration parameter. The estimated states by the no-discrepancy calibration model (shown in the lower left panel) has relatively large error. This is not surprising as the Lorenz-96 system is a misspecified model. The predictive mean of GaSP and S-GaSP by including both the calibrated computer model and discrepancy function are more accurate, as both model captures the discrepancy between the reality and computer model. Note that the estimation error of all models are larger than the ones when there is no discrepancy. This is because the measure error is large and we only observe 2 states at each time points. Increasing the number of observations or reducing the variance of measurement error can improve predictive accuracy.

## Concluding remarks

We have introduced the **RobustCalibration** package for Bayesian model calibration and data inversion. This package has implemented a range estimation methods and models, such as posterior sampling and MLE, for no-discrepancy calibration, GaSP and S-GaSP models of the discrepancy function. We implement statistical emulators for approximating computationally expensive computer models with both scalar-valued output or vectorized output. The package is applicable to observations from a single source with or without replications, and to observations from multiple sources or having different types. We illustrate our approaches on mathematical models with closed-form expressions or written as differential equations.

Even if we tried our best to consider different possible scenarios, a comprehensive statistical package for model calibration and data inversion is an ambitious goal. We will keep improving **RobustCalibration** package towards a few directions. First, we will make this package more computationally scalable on structured data, such as imaging and time series observations. Some computationally efficient methods of GaSP will be implemented in the **FastGaSP** package available on CRAN, and that will be called as a fast computing component by the **RobustCalibration** package in the future. Second, for problems like the Lorzen-96 system, it may be important to emulate the time evolution operator, if forecasting is our goal. Furthermore, we avoid recording posterior samples of the discrepancy due to constraints of storage and computational cost. Obtaining the uncertainty of the discrepancy function on test inputs may involve sampling the discrepancy functions. Finally, we will allow users to specify other prior of the parameters and proposal distributions for posterior samples in future versions of the package.

## Appendix

### Auxiliary facts

1. Let  $\tilde{\mathbf{R}}_{\gamma,\eta} = \mathbf{R}_\gamma/\eta + \mathbf{\Lambda}$  be an  $n \times n$  positive definite matrix as a function of parameters  $\gamma$  and  $\eta$ . Then for  $l = 1, \dots, p_x$

$$\frac{\partial \log |\tilde{\mathbf{R}}_{\gamma,\eta}|}{\partial \gamma_l} = \text{tr} \left( \frac{\tilde{\mathbf{R}}_{\gamma,\eta}^{-1}}{\eta} \frac{\partial \mathbf{R}_\gamma}{\partial \gamma_l} \right) \quad \text{and} \quad \frac{\partial \log |\tilde{\mathbf{R}}_{\gamma,\eta}|}{\partial \eta} = -\text{tr} \left( \frac{\tilde{\mathbf{R}}_{\gamma,\eta}^{-1} \mathbf{R}_\gamma}{\eta^2} \right).$$

2. Let  $\mathbf{H}$  be an  $n \times q$  full rank matrix with  $q < n$ ,  $\mathbf{Q} = \left( \tilde{\mathbf{R}}_{\gamma,\eta}^{-1} - \tilde{\mathbf{R}}_{\gamma,\eta}^{-1} \mathbf{H}^T (\mathbf{H}^T \tilde{\mathbf{R}}_{\gamma,\eta}^{-1} \mathbf{H})^{-1} \mathbf{H}^T \tilde{\mathbf{R}}_{\gamma,\eta}^{-1} \right)$  with  $\tilde{\mathbf{R}}_{\gamma,\eta} = \mathbf{R}_\gamma/\eta + \mathbf{\Lambda}$  and  $\mathbf{y}$  is an  $n \times 1$  vector. Then for  $l = 1, \dots, p_x$

$$\frac{\partial \log (\mathbf{y}^T \mathbf{Q}_{\gamma,\eta} \mathbf{y})}{\partial \gamma_l} = -\frac{\mathbf{y}^T \mathbf{Q}_{\gamma,\eta} \frac{\partial \mathbf{R}_\gamma}{\partial \gamma_l} \mathbf{Q}_{\gamma,\eta} \mathbf{y}}{\eta \mathbf{y}^T \mathbf{Q}_{\gamma,\eta} \mathbf{y}} \quad \text{and} \quad \frac{\partial \log (\mathbf{y}^T \mathbf{Q}_{\gamma,\eta} \mathbf{y})}{\partial \eta} = \frac{\mathbf{y}^T \mathbf{Q}_{\gamma,\eta} \mathbf{R}_\gamma \mathbf{Q}_{\gamma,\eta} \mathbf{y}}{\eta^2 \mathbf{y}^T \mathbf{Q}_{\gamma,\eta} \mathbf{y}}.$$

3. Suppose  $\mathbf{v}_\theta$  is an  $n \times 1$  vector as a function of  $\theta$  and  $\tilde{\mathbf{R}}$  is an  $n \times n$  positive definite matrix. Then for  $i = 1, \dots, p_\theta$

$$\frac{\partial \log (\mathbf{v}_\theta^T \tilde{\mathbf{R}}^{-1} \mathbf{v}_\theta)}{\partial \theta_i} = \frac{2 \mathbf{v}_\theta^T \tilde{\mathbf{R}}^{-1} \frac{\partial \mathbf{v}_\theta}{\partial \theta_i}}{\mathbf{v}_\theta^T \tilde{\mathbf{R}}^{-1} \mathbf{v}_\theta}.$$

### Likelihood functions and posterior distributions

**Posterior distribution of the no-discrepancy calibration.** Using the objective prior for the mean and variance parameters,  $\pi(\boldsymbol{\theta}_m, \sigma_0^2) \propto 1/\sigma_0^2$ , full conditional posterior distributions of the trend and variance parameters follow

$$\begin{aligned} \sigma_0^{-2} \mid \boldsymbol{\theta}_m, \boldsymbol{\theta} &\sim \text{Gamma} \left( \frac{n}{2}, \frac{(\mathbf{y}^F - \mathbf{f}_\theta^M - \mathbf{H}\boldsymbol{\theta}_m)^T \boldsymbol{\Lambda}^{-1} (\mathbf{y}^F - \mathbf{f}_\theta^M - \mathbf{H}\boldsymbol{\theta}_m)}{2} \right), \\ \boldsymbol{\theta}_m \mid \sigma_0^2, \boldsymbol{\theta} &\sim \mathcal{N} \left( \hat{\boldsymbol{\theta}}_m^{LS}, \sigma_0^{-2} (\mathbf{H}^T \boldsymbol{\Lambda}^{-1} \mathbf{H})^{-1} \right) \end{aligned}$$

The posterior distribution of the calibration parameters follows

$$p(\boldsymbol{\theta} \mid \boldsymbol{\theta}_m, \sigma_0^2, \boldsymbol{\beta}, \eta) \propto \exp \left( -\frac{(\mathbf{y}^F - \mathbf{f}_\theta^M - \mathbf{H}\boldsymbol{\theta}_m)^T \boldsymbol{\Lambda}^{-1} (\mathbf{y}^F - \mathbf{f}_\theta^M - \mathbf{H}\boldsymbol{\theta}_m)}{2\sigma_0^2} \right) \pi(\boldsymbol{\theta}),$$

where  $\pi(\boldsymbol{\theta})$  is the prior of calibration parameters where the default prior distribution is the uniform distribution  $\pi(\boldsymbol{\theta}) \propto 1$ . We use a Metropolis algorithm to sample the calibration parameters. Here we samples all calibration parameters as a block, instead of sequentially, as we only need to compute the likelihood once in block sampling. The proposal distribution of each coordinate of the calibration parameter vector is chosen as a normal distribution centered around a pre-specified standard deviation proportional to the range of the parameters. The default proportion is 0.05, and users can adjust the proportion by changing the first  $p_\theta$  value in the argument `sd_proposal` in `rcalibration` function. If, for instance, the proportion of accepted calibration parameters is too low, one can reduce the first  $p_\theta$  value in the argument `sd_proposal` to use a smaller standard deviation in the proposal distribution.

After obtaining  $S$  posterior samples with the first  $S_0$  burn-in samples, the predictive mean of reality based on calibrated computer model and trend by the no-discrepancy calibration can be computed by

$$\hat{\mu}(\mathbf{x}^*) = \frac{1}{S - S_0} \sum_{i=S_0+1}^S f^M(\mathbf{x}^*, \boldsymbol{\theta}^{(i)}) + \mathbf{h}(\mathbf{x}^*) \boldsymbol{\theta}_m^{(i)}.$$

The posterior credible interval of the reality  $y^R(\mathbf{x}^*)$  in no-discrepancy calibration can be obtained by the empirical quantile of posterior samples  $f^M(\mathbf{x}^*, \boldsymbol{\theta}^{(i)}) + \mathbf{h}(\mathbf{x}^*) \boldsymbol{\theta}_m^{(i)}$ . For example, the posterior credible interval of  $1 - \alpha$  percentile of the data  $f^M(\mathbf{x}^*)$  in no-discrepancy calibration can be computed by

$$\frac{1}{S - S_0} \sum_{i=S_0+1}^S f^M(\mathbf{x}^*, \boldsymbol{\theta}^{(i)}) + \mathbf{h}(\mathbf{x}^*) \boldsymbol{\theta}_m^{(i)} + \sqrt{\frac{\sigma_0^{(i)}}{w^*}} Z_\alpha$$

where  $Z_\alpha$  is an upper  $\alpha$  quantile of the standard normal distribution and  $w^*$  is the relative test output weight (assumed to be 1 by default).

**Likelihood function and derivatives in GaSP calibration.** The profile likelihood function in GaSP calibration follows

$$\mathcal{L}_K(\boldsymbol{\theta}, \gamma, \eta \mid \hat{\boldsymbol{\theta}}_m, \hat{\sigma}_0^2) \propto |\tilde{\mathbf{R}}|^{-\frac{1}{2}} (S_K^2)^{-\frac{n}{2}}. \quad (18)$$

where  $S_K^2 = (\mathbf{y} - \mathbf{f}_\theta^M - \mathbf{H}^T \hat{\boldsymbol{\theta}}_m)^T \tilde{\mathbf{R}}^{-1} (\mathbf{y} - \mathbf{f}_\theta^M - \mathbf{H}^T \hat{\boldsymbol{\theta}}_m)$ .

Denote  $\mathbf{v}_{\boldsymbol{\theta}_m} := (\mathbf{y} - \mathbf{f}_\theta^M - \mathbf{H}^T \hat{\boldsymbol{\theta}}_m)$ . Similar to the no-discrepancy calibration, we call the `lbfgs` function in the `nloptr` package (Ypma (2014)) for optimization. By facts 1 and 3, directly differentiating the profile likelihood function with respect to kernel and nugget parameters in (18) gives the following formulas not zero:

$$\begin{aligned} \frac{\partial \log(\mathcal{L}_K(\boldsymbol{\theta}, \gamma, \eta, \mid \hat{\boldsymbol{\theta}}_m, \hat{\sigma}^2))}{\partial \gamma_l} &= -\frac{1}{2} \text{tr} \left( \frac{\tilde{\mathbf{R}}_{\gamma, \eta}^{-1}}{\eta} \frac{\partial \mathbf{R}_\gamma}{\partial \gamma_l} \right) + \frac{n}{2} \times \frac{\mathbf{v}_{\boldsymbol{\theta}_m}^T \mathbf{Q}_{\gamma, \eta} \frac{\partial \mathbf{R}_\gamma}{\partial \gamma_l} \mathbf{Q}_{\gamma, \eta} \mathbf{v}_{\boldsymbol{\theta}_m}}{\eta \mathbf{v}_{\boldsymbol{\theta}_m}^T \mathbf{Q}_{\gamma, \eta} \mathbf{v}_{\boldsymbol{\theta}_m}} \\ \frac{\partial \log(\mathcal{L}_K(\boldsymbol{\theta}, \gamma, \eta, \mid \hat{\boldsymbol{\theta}}_m, \hat{\sigma}^2))}{\partial \eta} &= \frac{1}{2} \text{tr} \left( \frac{\tilde{\mathbf{R}}_{\gamma, \eta}^{-1} \mathbf{R}_\gamma}{\eta^2} \right) + \frac{n}{2} \times \frac{\mathbf{v}_{\boldsymbol{\theta}_m}^T \mathbf{Q}_{\gamma, \eta} \mathbf{R}_\gamma \mathbf{Q}_{\gamma, \eta} \mathbf{v}_{\boldsymbol{\theta}_m}}{\eta^2 \mathbf{v}_{\boldsymbol{\theta}_m}^T \mathbf{Q}_{\gamma, \eta} \mathbf{v}_{\boldsymbol{\theta}_m}} \\ \frac{\partial \log(\mathcal{L}_K(\boldsymbol{\theta}, \gamma, \eta, \mid \hat{\boldsymbol{\theta}}_m, \hat{\sigma}^2))}{\partial \theta_l} &= \frac{n}{2} \times \frac{\mathbf{v}_{\boldsymbol{\theta}_m}^T \mathbf{Q}_{\gamma, \eta} \frac{\partial \mathbf{f}_\theta^M}{\partial \theta_l}}{\mathbf{v}_{\boldsymbol{\theta}_m}^T \mathbf{Q}_{\gamma, \eta} \mathbf{v}_{\boldsymbol{\theta}_m}} \end{aligned}$$

for  $l = 1, \dots, p_x$  and  $i = 1, \dots, p_\theta$ . When the mean function is zero, one can simply replace  $\mathbf{Q}_{\gamma, \eta}$  by  $\tilde{\mathbf{R}}_{\gamma, \eta}$  in the formula above to obtain the derivatives. Besides, when  $\frac{\partial \mathbf{f}_\theta^M}{\partial \theta_l}$  is not available, we use the numerical derivatives to approximate.

**Posterior distributions in GaSP calibration.** After marginalizing out the discrepancy function, the marginal distribution follows  $\mathbf{y}^F \sim \mathcal{MN}(\mathbf{f}_\theta^M + \mathbf{H}\boldsymbol{\theta}_m, \sigma_0^2 \tilde{\mathbf{R}})$ , where  $\tilde{\mathbf{R}} = \mathbf{R}/\eta + \boldsymbol{\Lambda}$ . We assume the object prior for the mean and noise variance parameters  $\pi(\boldsymbol{\theta}_m, \sigma_0^2) \propto 1/\sigma_0^2$ . Full conditional posterior distributions of the trend and variance parameters follow

$$\begin{aligned} \sigma_0^{-2} \mid \boldsymbol{\theta}_m, \boldsymbol{\theta} &\sim \text{Gamma} \left( \frac{n}{2}, \frac{(\mathbf{y}^F - \mathbf{f}_\theta^M - \mathbf{H}\boldsymbol{\theta}_m)^T \tilde{\mathbf{R}}^{-1} (\mathbf{y}^F - \mathbf{f}_\theta^M - \mathbf{H}\boldsymbol{\theta}_m)}{2} \right), \\ \boldsymbol{\theta}_m \mid \sigma_0^2, \boldsymbol{\theta} &\sim \mathcal{MN} \left( \hat{\boldsymbol{\theta}}_m, \sigma_0^{-2} (\mathbf{H}^T \tilde{\mathbf{R}}^{-1} \mathbf{H})^{-1} \right), \end{aligned}$$

where  $\hat{\boldsymbol{\theta}}_m = (\mathbf{H}^T \tilde{\mathbf{R}}^{-1} \mathbf{H})^{-1} \mathbf{H}^T \tilde{\mathbf{R}}^{-1} (\mathbf{y} - \mathbf{f}_\theta^M)$ . Since the full conditional distributions are known, a Gibbs sampler is used to sample  $\sigma_0^{-2}$  and  $\boldsymbol{\theta}_m$  from the full conditional distribution.

Given the trend and variance parameter, the conditional distribution of the calibration parameters

follows

$$p(\boldsymbol{\theta} \mid \boldsymbol{\theta}_m, \sigma^2) \propto \exp\left(-\frac{(\mathbf{y}^F - \mathbf{f}_\theta^M - \mathbf{H}\boldsymbol{\theta}_m)^T \tilde{\mathbf{R}}^{-1}(\mathbf{y}^F - \mathbf{f}_\theta^M - \mathbf{H}\boldsymbol{\theta}_m)}{2\sigma_0^2}\right) \pi(\boldsymbol{\theta}),$$

We implement the Metropolis algorithm with the proposal distribution being a normal distribution with the mean centered around the current value of the posterior sample. Users can adjust the standard deviation of the proposal distribution by argument `sd_proposal` in the `rcalibration` function.

Denote the inverse range parameter  $\beta_l = 1/\gamma_l$ ,  $l = 1, \dots, p_x$ . The conditional distribution of the inverse range and nugget parameters follow

$$p(\boldsymbol{\beta}, \eta \mid \boldsymbol{\theta}, \boldsymbol{\theta}_m, \sigma_0^2) \propto |\tilde{\mathbf{R}}|^{-\frac{n}{2}} \exp\left(-\frac{(\mathbf{y}^F - \mathbf{f}_\theta^M - \mathbf{H}\boldsymbol{\theta}_m)^T \tilde{\mathbf{R}}^{-1}(\mathbf{y}^F - \mathbf{f}_\theta^M - \mathbf{H}\boldsymbol{\theta}_m)}{2\sigma_0^2}\right) \pi(\boldsymbol{\gamma}, \eta),$$

where we assume the prior for the range and nugget parameters follows the jointly robust (JR) prior (Gu, 2018)

$$\pi(\boldsymbol{\beta}, \eta) = C \left( \sum_{l=1}^{p_x} C_l \beta_l + \eta \right)^a \exp\left\{-b \left( \sum_{l=1}^{p_x} C_l \beta_l + \eta \right)\right\}$$

where  $C$  is normalizing constant. By default, we use the following prior parameters  $a = 1/2 - p_x$ ,  $b = 1$ , and  $C_l = n^{-1/p_x} |x_l^{max} - x_l^{min}|$ , with  $x_l^{max}$  and  $x_l^{min}$  being the maximum and minimum values of the observable input at the  $l$ th coordinate. Users can adjust  $a$  and  $b$  in the `rcalibration` function. The JR prior is a proper prior. Furthermore, the default choices of prior parameters induces a small penalty on very large correlation, preventing the identifiability issues of the calibration parameters due to large correlation (Gu, 2018).

Since the posterior distribution is not a known distribution, we use the Metropolis algorithm to sample the logarithm of the inverse range parameter  $\log(\boldsymbol{\beta})$  and nugget parameter  $\log(\eta)$ . The proposal distribution of each parameter is a normal distribution centered around the current value and with a pre-specified standard deviation chosen to be 0.25 by default. User can change the  $p_\theta + 1$  to  $p_x + p_\theta + 1$  coordinates of the vector in the argument `sd_proposal` in the `rcalibration` function to specify the standard deviation in the proposal distribution for these parameters.

**Likelihood function and posterior distributions S-GaSP calibration.** The likelihood function and posterior distribution of S-GaSP follow from the those in GaSP calibration, by simply replacing the kernel  $K$  to  $K_{Z_d}$  in Table 1.

## Acknowledgements

This research was supported by the National Science Foundation under Award Number DMS-2053423. We thank Xubo Liu for implementing the numerical method for simulating the Lorenz 96 model.

## Bibliography

- P. Agram and M. Simons. A noise model for InSAR time series. *Journal of Geophysical Research: Solid Earth*, 120(4):2752–2771, 2015. [p12]
- K. R. Anderson, I. A. Johanson, M. R. Patrick, M. Gu, P. Segall, M. P. Poland, E. K. Montgomery-Brown, and A. Miklius. Magma reservoir failure and the onset of caldera collapse at Kilauea volcano in 2018. *Science*, 366(6470), 2019. [p3, 10, 12, 13]
- P. D. Arendt, D. W. Apley, and W. Chen. Quantification of model uncertainty: calibration, model discrepancy, and identifiability. *Journal of Mechanical Design*, 134(10):100908, 2012. [p1]
- M. Bayarri, J. Berger, J. Cafeo, G. Garcia-Donato, F. Liu, J. Palomo, R. Parthasarathy, R. Paulo, J. Sacks, and D. Walsh. Computer model validation with functional output. *The Annals of Statistics*, 35(5): 1874–1906, 2007a. [p1]
- M. J. Bayarri, J. O. Berger, R. Paulo, J. Sacks, J. A. Cafeo, J. Cavendish, C.-H. Lin, and J. Tu. A framework for validation of computer models. *Technometrics*, 49(2):138–154, 2007b. [p2, 4, 6, 8, 9, 11]
- G. Box and G. Coutie. Application of digital computers in the exploration of functional relationships. *Proceedings of the IEE-Part B: Radio and Electronic Engineering*, 103(1S):100–107, 1956. [p11]

- J. Brajard, A. Carrassi, M. Bocquet, and L. Bertino. Combining data assimilation and machine learning to emulate a dynamical model from sparse and noisy observations: A case study with the Lorenz 96 model. *Journal of Computational Science*, 44:101171, 2020. [p16]
- M. Carmassi, P. Barbillon, M. Chiodetti, M. Keller, and E. Parent. Calico: a r package for bayesian calibration. *arXiv preprint arXiv:1808.01932*, 2018. [p3, 10]
- W. Chang, M. Haran, P. Applegate, and D. Pollard. Calibrating an ice sheet model using high-dimensional binary spatial data. *Journal of the American Statistical Association*, 111(513):57–72, 2016. [p1]
- M. Gu. Jointly robust prior for Gaussian stochastic process in emulation, calibration and variable selection. *Bayesian Analysis*, 14(1), 2018. [p7, 20]
- M. Gu and K. Anderson. Calibration of imperfect mathematical models by multiple sources of data with measurement bias. *arXiv preprint arXiv:1810.11664*, 2018. [p12]
- M. Gu and J. O. Berger. Parallel partial Gaussian process emulation for computer models with massive output. *Annals of Applied Statistics*, 10(3):1317–1347, 2016. [p10, 12]
- M. Gu and L. Wang. Scaled Gaussian stochastic process for computer model calibration and prediction. *SIAM/ASA Journal on Uncertainty Quantification*, 6(4):1555–1583, 2018. [p2, 8, 9]
- M. Gu, X. Wang, and J. O. Berger. Robust Gaussian stochastic process emulation. *Annals of Statistics*, 46(6A):3038–3066, 2018a. [p10]
- M. Gu, F. Xie, and L. Wang. A theoretical framework of the scaled Gaussian stochastic process in prediction and calibration. *arXiv preprint arXiv:1807.03829*, 2018b. [p2, 9]
- M. Gu, J. Palomo, and J. O. Berger. RobustGaSP: Robust Gaussian Stochastic Process Emulation in R. *The R Journal*, 2019. [p3, 10]
- R. K. Hankin. Introducing BACCO, an R bundle for Bayesian analysis of computer code output. *Journal of Statistical Software*, 14:1–21, 2005. [p3]
- D. Higdon, J. Gattiker, B. Williams, and M. Rightley. Computer model calibration using high-dimensional output. *Journal of the American Statistical Association*, 103(482):570–583, 2008. [p1]
- M. C. Kennedy and A. O’Hagan. Bayesian calibration of computer models. *Journal of the Royal Statistical Society: Series B (Statistical Methodology)*, 63(3):425–464, 2001. [p1, 3]
- H. Li and M. Gu. Robust estimation of SARS-CoV-2 epidemic in us counties. *Scientific reports*, 11(1):1–16, 2021. [p11]
- D. C. Liu and J. Nocedal. On the limited memory bfgs method for large scale optimization. *Mathematical programming*, 45(1-3):503–528, 1989. [p4]
- F. Liu, M. Bayarri, and J. Berger. Modularization in Bayesian analysis, with emphasis on analysis of computer models. *Bayesian Analysis*, 4(1):119–150, 2009. [p11]
- E. N. Lorenz. Predictability: A problem partly solved. In *Proc. Seminar on predictability*, volume 1, 1996. [p11, 15]
- B. MacDonald, P. Ranjan, H. Chipman, et al. Gpfit: An R package for fitting a Gaussian process model to deterministic simulator outputs. *Journal of Statistical Software*, 64(i12), 2015. [p3, 10]
- J. Maclean and E. T. Spiller. A surrogate-based approach to nonlinear, non-Gaussian joint state-parameter data assimilation. *arXiv preprint arXiv:2012.04793*, 2020. [p16]
- J. Nocedal. Updating quasi-Newton matrices with limited storage. *Mathematics of computation*, 35(151):773–782, 1980. [p4]
- J. Palomo, R. Paulo, G. García-Donato, et al. Save: an R package for the statistical analysis of computer models. *Journal of Statistical Software*, 64(13):1–23, 2015. [p3, 10]
- R. Paulo, G. García-Donato, and J. Palomo. Calibration of computer models with multivariate output. *Computational Statistics and Data Analysis*, 56(12):3959–3974, 2012. [p1]
- M. Plumlee. Bayesian calibration of inexact computer models. *Journal of the American Statistical Association*, 112(519):1274–1285, 2017. [p2]

- O. Roustant, D. Ginsbourger, and Y. Deville. Dicekriging, Diceoptim: Two R packages for the analysis of computer experiments by kriging-based metamodeling and optimization. *Journal of Statistical Software*, 51(1):1–55, 2012. ISSN 1548-7660. [p3, 10]
- J. Sacks, W. J. Welch, T. J. Mitchell, H. P. Wynn, et al. Design and analysis of computer experiments. *Statistical science*, 4(4):409–423, 1989. [p1, 10]
- T. J. Santner, B. J. Williams, and W. I. Notz. *The design and analysis of computer experiments*. Springer Science & Business Media, 2003. [p10]
- N. A. Simakov, R. L. Jones-Ivey, A. Akhavan-Safaei, H. Aghakhani, M. D. Jones, and A. K. Patra. Modernizing titan2d, a parallel amr geophysical flow code to support multiple rheologies and extendability. In *International Conference on High Performance Computing*, pages 101–112. Springer, 2019. [p10]
- K. Soetaert, T. Petzoldt, and R. W. Setzer. Solving differential equations in R: package desolve. *Journal of statistical software*, 33:1–25, 2010. [p11]
- R. Tuo and C. J. Wu. Efficient calibration for imperfect computer models. *The Annals of Statistics*, 43(6): 2331–2352, 2015. [p2]
- R. Tuo and C. J. Wu. A theoretical framework for calibration in computer models: parametrization, estimation and convergence properties. *SIAM/ASA Journal on Uncertainty Quantification*, 4(1):767–795, 2016. [p1, 2]
- H. Wickham. ggplot2. *Wiley Interdisciplinary Reviews: Computational Statistics*, 3(2):180–185, 2011. [p3]
- D. Williamson, M. Goldstein, L. Allison, A. Blaker, P. Challenor, L. Jackson, and K. Yamazaki. History matching for exploring and reducing climate model parameter space using observations and a large perturbed physics ensemble. *Climate dynamics*, 41(7-8):1703–1729, 2013. [p1]
- R. K. Wong, C. B. Storlie, and T. Lee. A frequentist approach to computer model calibration. *Journal of the Royal Statistical Society: Series B (Statistical Methodology)*, 79:635–648, 2017. [p2]
- J. Ypma. *nloptr: R interface to NLOpt*, 2014. URL <https://CRAN.R-project.org/package=nloptr>. R package version 1.0.4. [p4, 19]

Mengyang Gu  
Department of Statistics and Applied Probability  
University of California, Santa Barbara  
Santa Barbara, California, USA  
[mengyang@pstat.ucsb.edu](mailto:mengyang@pstat.ucsb.edu)